Chapter 4. Permeability, Diffusivity, and Solubility of Gas and Solute Through Polymers

Introduction

The diffusion of small molecules into polymers is a function of both the polymer and the diffusant. Factors which influence diffusion include: (1) the molecular size and physical state of the diffusant; (2) the morphology of the polymer; (3) the compatibility or solubility limit of the solute within the polymer matrix; (4) the volatility of the solute; (5) and the surface or interfacial energies of the monolayer films (*1-4*). Researchers have attempted to explain specific mechanisms by which diffusion occurs in polymeric systems, but there is no unified theory to explain this phenomenon (*5*).

Formulation of the gas transport phenomena through polymer membranes is directed in two areas: (1) development of quantitative theories based on the thermodynamics and kinetic properties of the gas-polymer system, and (2) experimental study of gas transport through various polymers. Most quantitative theories are primarily based on regular polymer solution theories. Empirical studies observe behaviors for gas-polymer systems and then correlate these findings to known phenomenological models. Based on the focus of these empirical studies, either microscopic (molecular) or macroscopic (continuum) theories are employed (*6*).

Theory of Gas Permeation and Diffusion Through Polymer Membranes

Fundamentals

The first study of gas permeation through a polymer was conducted by Thomas Graham in 1829 (*7*). Graham observed a loss in volume of a wet pig bladder inflated with CO_2. In 1866, Graham formulated the solution diffusion process, where he postulated that the permeation process involved the dissolution of penetrant, followed by transmission of the dissolved species through the membrane. The other important observations made at the time were:

1) Permeation was independent of pressure.
2) Increase in temperature lead to decrease in penetrant solubility, but made the membrane more permeable.
3) Prolonged exposure to elevated temperature affected the retention capacity of the membrane.

4) Differences in the permeability could be exploited for application in gas separations.
5) Variation in membrane thickness altered the permeation rate but not the separation characteristics of the polymer.

Fick in 1855, by analogy to Fourier's law of heat conduction, proposed the law of mass diffusion which is stated as, …"the mathematical theory of diffusion in isotropic substances is based on the hypothesis that the rate of transfer of diffusing substances through unit area of a section is proportional to the concentration gradient measured normal to the section" (*8*). Fick's first law of diffusion is mathematically expressed as:

$$J \text{ or F or q} = -D\frac{\partial C}{\partial x'} \tag{1}$$

where *J, F,* or *q* is the rate of transfer per unit area of section, *C* is the concentration of diffusing substances, and *x* is the space co-ordinate measured normal to the section. If *F* and *C* are both expressed in terms of the same unit of quantity, *D* is then independent of the unit and has dimensions length^2 time^{-1}.

Once the mass-balance of an element is taken into account, equation (1) can be used to derive the fundamental differential equation of diffusion: (*8*)

$$\frac{\partial C}{\partial t} = D\left(\frac{\partial^2 C}{\partial x^2} + \frac{\partial^2 C}{\partial y^2} + \frac{\partial^2 C}{\partial z^2}\right). \tag{2}$$

In polymeric and non-homogeneous systems, the diffusion coefficient largely depends on the concentration. The diffusion coefficient in polymeric and non-homogeneous systems varies from point to point and equation (2) is more accurately expressed: (*8*)

$$\frac{\partial C}{\partial t} = \frac{\partial}{\partial x}\left(D\frac{\partial C}{\partial x}\right) + \frac{\partial}{\partial y}\left(D\frac{\partial C}{\partial y}\right) + \frac{\partial}{\partial z}\left(D\frac{\partial C}{\partial z}\right) \tag{3}$$

where D is a function of x, y, z and C. In most applications, diffusion is restricted to one direction. For example, many times a gradient of concentration is present and diffusion only occurs along the x-axis. In these cases, equations (2) and (3) can be reduced to: (*8*)

$$\frac{\partial C}{\partial t} = D\frac{\partial^2 C}{\partial x^2} \tag{4}$$

and

$$\frac{\partial C}{\partial t} = \frac{\partial}{\partial x}\left(D\frac{\partial C}{\partial x} \right) \text{ , respectively.} \tag{5}$$

Equations (4) and (5) are commonly referred to as Fick's second law of diffusion.

In the late 1870's, Stefan and Exner demonstrated that gas permeation through a soap membrane was proportional to the product of solubility coefficient (S) and Fick's diffusion coefficient (D). Based on the findings of Stefan and Exner, von Wroblewski constructed a quantitative solution to the Graham's solution-diffusion model. The dissolution of gas was based on Henry's law of solubility, where the concentration of the gas in the membrane was directly proportional to the applied gas pressure: (*7*)

$$P = \frac{C}{S} \tag{6}$$

where P is the permeability coefficient.

Wroblewski further showed that under steady state conditions, and assuming diffusion and solubility coefficients to be independent of concentration, the gas permeation flux can be expressed as: (*7*)

$$J = D \cdot S \cdot \left(\frac{p_f - p_p}{l} \right) = P\left(\frac{\Delta p}{l} \right) \tag{7}$$

where (p_f) and (p_p) are the upstream and downstream pressures imposed on a membrane, ($\Delta p/l$) is the applied pressure gradient across the membrane thickness (l), and P is defined as the gas permeability of the membrane. A schematic representation of gas transport through a membrane is shown in Figure 1. The gas permeability of a membrane is often expressed in Barrers, where 1 Barrer = 10^{-10} (cm^3(STP) / cm. sec. cmHg).

In 1920, Daynes showed that it was impossible to evaluate both diffusion and solubility coefficients by steady-state permeation experiments. He presented a mathematical solution using Fick's second law of diffusion, equations (4) and (5), for calculating the diffusion coefficient, which was assumed to be independent of concentration: (*7*)

$$\frac{\partial C}{\partial t} = D\frac{\partial^2 C}{\partial x^2}. \tag{8}$$

This "time lag method" is still the most common method for estimating the gas diffusion coefficient.

Permeation Models and Methods of Calculation

Steady State Model

Many mathematical models used to describe diffusion assume steady state conditions. Steady state conditions assume that diffusant concentrations remain constant at all points on each side or surface of a plastic sheet or membrane. Provided the diffusion coefficient is constant, Fick's second law of diffusion, equation (4), reduces to: (*8*)

$$\frac{d^2 C}{dx^2} = 0. \tag{9}$$

Integrating equation (9) twice with respect to x and introducing the conditions at x=0 and l, one obtains: (*8*)

$$\frac{C - C_1}{C_2 - C_1} = \frac{x}{l}. \tag{10}$$

The concentration changes linearly from C_1 to C_2 through a plastic sheet or membrane and the rate of transfer for a diffusing substance is the same across all sections. Therefore, the rate of transfer per unit area of section is calculated by: (*8*)

$$J = -D\frac{dC}{dx} = \frac{D(C_1 - C_2)}{l}. \tag{11}$$

If the thickness and the surface concentrations of the diffusant are known, the diffusion coefficient can be extrapolated from flow rate.

In systems where a gas or vapor is the diffusant, the surface concentration may not be known. In gas and vapor systems, the rate of diffusant transfer is expressed in terms of vapor pressures, ρ_1, ρ_2, by the following equation: (*8*)

$$J = \frac{P(\rho_1 - \rho_2)}{l} \tag{12}$$

where P is the permeability coefficient. Henry's law of solubility, equation (6), states that a linear relationship exists between the external vapor pressure and the corresponding concentration within the surface of the plastic sheet or membrane (*8*). The relationship in equation (6) is commonly extrapolated from a linear sorption isotherm. If one assumes the diffusion coefficient to be constant, the relationship between the diffusion coefficient, the permeation coefficient, and the solubility coefficient simplifies to: (*8*).

$$P = D \cdot S. \tag{13}$$

In closing, if the rate of diffusion is empirically determined and the solubility coefficient for the diffusant is known, the permeation and diffusion coefficients are easily calculated from equations (12) and (13).

Time Lag Method Assuming a Constant Diffusion Coefficient

Prior to the establishment of steady state conditions, the rate of flow and the concentration of a diffusant at any point of the sheet vary with time. If one assumes the diffusion coefficient to be constant, the plastic sheet or membrane is initially completely free of diffusant and diffusant is continually removed from the low concentration side (C_2=0), the amount of diffusant, Q_t, which passes through the sheet in time, t, is given by: (*8*)

$$\frac{Q_t}{lC_1} = \frac{Dt}{l^2} - \frac{1}{6} - \frac{2}{\pi^2}\sum_1^{\infty}\frac{(-1)^n}{n^2} exp\left(\frac{-Dn^2\pi^2 t}{l^2}\right). \tag{14}$$

As steady state is approached, $t \rightarrow \infty$, the exponential terms become negligibly small, allowing for plotting Q_t versus t: (*8*)

$$Q_t = \frac{DC_1}{l}\cdot\left(t - \frac{l^2}{6D}\right). \tag{15}$$

The intercept, L', on the t-axis is given by: (*8*)

$$L' = \frac{l^2}{6D}. \tag{16}$$

The diffusion coefficient can be calculated from equation (16) upon obtainment of L'. Permeability and solubility can be subsequently calculated using previously discussed equations (12) and (13), respectively.

Time Lag Method Assuming a Variable Diffusion Coefficient

Frisch (1957) described expressions for the time lag in linear diffusion through a sheet or membrane with a concentration-dependent diffusion coefficient. The relationship between the diffusion coefficient and the diffusant concentration must be known or calculated from an arbitrary expression containing unknown parameters. The dependence of the diffusion

coefficient on the concentration of the diffusant is usually represented by the following equation: (*9,10*)

$$D = D_0 e^{\beta C} \tag{17}$$

where β is a constant, and D_0 is the diffusion coefficient as concentration approaches zero. The values of β and D_0 are determined from a series of measurements of the time lag.

Sorption and Desorption Kinetics

The rate of gas sorption can be used to estimate the diffusion coefficient of a gas. The measurement of this transport rate can also be used to study relative mobility rates of a penetrant and the polymer chain during the sorption process (*11*). The relative mobility is classified as Case I (Fickian) or Case II (anomalous or non-Fickian) sorption. The sorption cycles for these transport mechanisms are shown in Figure 2. Case I sorption occurs when the penetrant-polymer system obeys Fickian diffusion, where the mobility of the penetrant is slower than the polymer chain mobility. In case I sorption, the rate of penetrant mass uptake is proportional to the square root of time. The empirical mathematical correlations presented below are all based on Case I sorption kinetics. In case II sorption, the rate of mass uptake is directly proportional to time. Penetrant diffusion rate is faster than the chain mobility, thereby leading to swelling of the polymer. Anomalous sorption occurs during comparable mobility of both the penetrant and the polymer chain. Due to the complex nature of the sorption kinetics, this behavior is termed either anomalous or non-Fickian.

Constant Diffusion Coefficient

In his seminal work, Crank proposed a classical Fickian diffusion model which links the mass of diffusant (M) with time (t) for a specific thickness of film (l) (*12*). If the concentration of the diffusant is assumed to be initially uniform within the sheet, and the surface concentration is immediately brought to zero, Fick's second law, equation (4), can be expressed by the following equations: (*8,10,13*)

$$\frac{M_t}{M_\infty} = 1 - \sum_{n=0}^{\infty} \frac{8}{(2n+1)^2 \pi^2} \exp\left[-D(2n+1)^2 \pi^2 t / l^2\right] \tag{18}$$

$$\frac{M_t}{M_\infty} = 4\left(\frac{Dt}{l^2}\right)^{1/2} \cdot \left[\frac{1}{\pi^{1/2}} + 2\sum_{n=0}^{\infty} (-1)^n \, ierfc \frac{nl}{2(Dt)^{1/2}}\right] \tag{19}$$

where M_t is the amount of migrant lost by a polymer at time t and M_∞ is the final amount of migrant lost until equilibrium is reached. The diffusion coefficient can be graphically extrapolated by an observation of the initial gradient of a graph of M_t/M_∞ as a function of $(t/l^2)^{1/2}$. In cases where the diffusion coefficient is constant, the graph for a sorption experiment is a straight line. "If the diffusion coefficient is a function of concentration which increases as concentration increases, the graph is linear over an even larger increase in M_t"(*8*).

For $M_t/M_\infty > 0.6$, equation (18) can be accurately replaced by equation (20): (*13*)

$$\frac{M_t}{M_\infty} = 1 - \frac{8}{\pi^2} \exp\left(\frac{-\pi^2 Dt}{l^2}\right). \tag{20}$$

For $M_t/M_\infty < 0.6$, equation (19) can be approximated with very little error by equations (21) or (22): (*10,13*)

$$\frac{M_t}{M_\infty} = 4\left(\frac{Dt}{\pi l^2}\right)^{1/2} \qquad = \tag{21}$$

$$\frac{M_t}{M_\infty} = \left(\frac{16D}{\pi l^2}\right)^{1/2} \cdot t^{1/2}. \tag{22}$$

Equations (18) and (20) are commonly used to describe long-term migration, whereas equations (19), (21) and (22) are used to describe relatively short-term migration (*13*).

For desorption experiments, equation (20) can be rearranged to: (*10*)

$$\ln\left(M_\infty - M_t\right) = \ln\left(\frac{8M_\infty}{\pi^2}\right) - \frac{\pi^2 D_0 t}{l^2} \tag{23}$$

where D_0 is the diffusion coefficient as the concentration approaches zero. Equation (23) shows that for large values of t a plot of $\ln(M_\infty - M_0)$ versus t gives a straight line with a slope of θ: (*10*)

$$\theta = -\frac{\pi^2 D_0}{l^2}. \tag{24}$$

The diffusion coefficient as concentration approaches zero, D_0, can be calculated from equation (24).

Diffusion is often expressed in terms of the time at which half of the equilibrium migrant has penetrated the sheet or membrane, (M_t/M_∞=0.5) is designated as $t_{1/2}$. Equations (20), (21) and (22) can be further reduced to the form: (*13*)

$$D = \frac{0.049 \cdot l^2}{t_{1/2}}. \tag{25}$$

Therefore, if the half-time of a sorption or desorption process is observed experimentally, the value of D, assumed constant, can be determined.

Concentration-dependent Diffusion Coefficients

The diffusion coefficient rarely remains constant or follows a linear relationship when plotting M_t/M_∞ as a function of $(t/l^2)^{1/2}$. Therefore, a series of sorption experiments covering a range of surface concentrations are commonly conducted to decipher how the diffusion coefficient is related to concentration given the initial-rates-of-sorption curves plotted against $(t/l^2)^{1/2}$ for a number of different surface concentrations (*8*).

Each sorption curve yields a variable diffusion coefficient. Based on these experimental sorption curves, an average variable diffusion coefficient, D', over a range of concentrations can

be determined. Crank (1975) has shown that for any one experiment the variable diffusion coefficient provides a reasonable approximation to:

$$D' = \frac{1}{C_0} \int_0^{C_0} D dC \,, \tag{26}$$

where 0 to C_0 is the concentration range existing in the sheet or membrane for a set of sorption curves in a particular experiment. The relationship between D and C can be obtained by extrapolating D' from a series of sorption experiments and equation (26) (*8*).

In cases where quantifying the permeation of a chemical through a polymeric membrane is the objective, the dependence of D on the concentration of the permeating species is usually represented by equation (17). Substitution of equation (17) into equation (26) and integration yields: (*10*)

$$D' = \frac{D_0}{C_0 \beta} \left(e^{\beta C_0} - 1 \right). \tag{27}$$

The diffusion coefficient of polymer-chemical systems as a function of concentration can be determined when D_0 and β are known. As previously discussed, these parameters can be calculated from desorption experiments as follows: (1) D' is calculated from the slope of the linear portion of the graph of M_t/M_∞ versus $t^{1/2}$; (2) D_0 is calculated from the slope of the graph of $\ln(M - M_\infty)$ versus t (for large values of t); and (3) β is calculated from equation (27) (*10*).

The steady-state rate of permeation of a chemical through a polymeric membrane can be found by the substitution of equation (17) into equation (1) and integration of the resulting expression: (*10*)

$$J = \frac{D_0}{\beta l} \left(e^{\beta C_0} - 1 \right). \tag{28}$$

Gas Permeation in Polymeric Materials

Gas permeation has been studied for over 150 years. However, significant advances in

the understanding of gas permeation have been made only in the last three decades. The interest in the field was generated from developments of new synthetic polymeric materials. The study of gas transport through polymer membranes is based on the morphology of the polymer. The gas transport through amorphous polymers is further divided into rubbery and glass polymer classifications.

Gas Permeation in Rubbery Polymers

Sorption

Gas solubility in rubbery polymers is well defined in terms of Henry's law of solubility, equation (6). This model is valid for low molecular weight gases and at low gas pressures. Positive deviations to this model are observed when swelling of the polymer matrix occurs in the presence of penetrants (*12*). The sorption of mixed gases in rubbery polymers is evaluated in terms of the partial solubility of the gas mixture. The partial pressure, and the Henry's law solubility coefficient value of each individual gas are used to calculate the partial solubility of the gas mixture (*14*).

Diffusion

The gas transport through rubbery polymers is described according to Fick's law for diffusion. The diffusion coefficient is known to be concentration independent whenever Henry's law of solubility is applicable (*12*). The permeate flux during mixed gas permeation is shown to be the sum of the permeate flux of individual gases, based on the partial pressure of gases. Therefore, the diffusion coefficient for mixed gas systems remains the same. Gas-gas interactions, as well as, gas-polymer interactions do not affect the diffusion coefficient of gases in rubbery polymers (*14*).

Gas Permeation in Glassy Polymers

Non-equilibrium Behavior

Models have been proposed to describe the observed transport behavior in glassy polymers based upon statistical, mechanical-structure, and thermodynamic considerations. These models fall into three basic theories (*6*).

1) The "hole" vacancy theory states that work is assumed to be done on the polymer matrix to create or expand a hole for the gas molecule. The successful creation and expansion leads to the diffusion of gas molecule through the membrane.
2) The activated complex theory describes the movement of gas molecules with sufficient energy through the matrix by overcoming a potential energy barrier.
3) The fluctuation theory is based on thermal fluctuations in the matrix leading to an emergence of excess space which then permits the passage of gas molecules.

The three theories discussed above are derived from the free volume molecular theory. This theory postulates that the movement of gas molecules is dependent upon the available free volume in the polymer matrix, as well as, sufficient energy of the gas molecules to overcome attractive forces between chains (*6*).

In 1960, Fujita proposed the presence of free volume within a polymer. The concept is based on the presence of three components for the specific volume of any polymer. The three components consist of: (1) the occupied volume of the macromolecules; (2) the interstitial free volume, which is small and is distributed uniformly throughout the material; and (3) the hole free volume, which is large enough to allow gas transport (*15*). The hole free volume is also referred to as the excess free volume.

The interstitial volume dependence on temperature is essential in defining the differences between the rubbery and glassy state of an amorphous polymer. The glass transition temperature is often defined as the point where the expansion coefficient of the polymer changes. The polymer below its glass transition temperature is treated as a solid and is termed a glassy polymer, whereas the polymer above its glass transition temperature is a rubbery polymer and exhibits viscous liquid like properties. Thus, a glass transition temperature of a polymer is highly dependent on the annealing process. The concept of free volume has been used to qualitatively describe the non-equilibrated nature of the polymer. The simplicity of the free volume theory, as being a single parameter model, has been an important reason for its wide application in gas transport studies through polymer membranes (*16*).

Fujita's free volume theory and subsequent theories for the same subject are largely based on an expression developed by Doolittle. Doolittle empirically described the temperature-dependence of the viscosity of simple liquids by the following equation: (*12*)

$$m_d = A_d \exp\left(\frac{-B_d}{v_f}\right) \tag{29}$$

where m_d is the mobility of the diffusant component relative to the polymer component, v_f is the average fractional free volume of the system, and A_d and B_d are parameters which are assumed to be independent of diffusant concentration and temperature. The usual definitions for v_f and m_d are shown in equations (30) and (31), respectively (*12*).

$$v_f = v_f(T_s, \pi_s, v = 0) + \alpha(T - T_s) - \beta(\pi - \pi_s) + \gamma v \tag{30}$$

The subscript 's' denotes a reference state and

α is the thermal expansion coefficient $\left(= \left(\frac{\partial v_f}{\partial T}\right)_s\right)$, (30.1)

β is the compressability $\left(= \left(\frac{\partial v_f}{\partial p}\right)_s\right)$, (30.2)

π and π_s are hydrostatic pressures, which are related to gas pressures, and

γ is the concentration coefficient $\left(= \left(\frac{\partial v_f}{\partial v}\right)_s\right)$. (30.3)

$$D_T = RTm_d \tag{31}$$

where D_T is the thermodynamic diffusion coefficient of the diffusant component relative to the polymer component, R is the gas constant and T is the absolute temperature of the system.

The diffusion coefficient is related to the thermodynamic diffusion coefficient by equation (32), where '*a*' is the activity of the gas. The fractional free volume is a measure of gas solubility in the polymer and is linearly related to the operating condition, i.e. temperature, pressure, and concentration (*17*).

$$D = D_T \left(\frac{\partial \ln a}{\partial \ln v} \right)_{T,p} \left(\frac{1}{1-v} \right) \tag{32}$$

Stern et al. (*17*) applied the free volume theory to study gas transport through polymers with moderate success. Fang (*18*) attempted to study binary gas transport through polymers in the same manner that Stern had done for single simple gases, but was unable to devise a valid model. The effect of a second component on the free volume is assumed to be additive, which then restricts the applicability of a model to dilute systems, where the penetration concentration is less than 0.2 volume fraction.

To explain the mechanism behind the transport of gas molecules through the free volume present in the polymer matrix, the gas polymer system is defined in terms of liquid molecules traveling through a liquid membrane. The Cohen and Turnbull theory, and Brandt theory, both proposed in 1959, considered transport through liquid molecules denoted as hard spheres (*12*). The Cohen and Turnbull model defined the diffusion as a redistribution of free volume within the liquid, whereas the model by Brandt described the process in terms of an activation energy barrier. Another theory proposed by Dibenedetto and Paul in 1963 used the same concept as that of Cohen and Turnbull regarding free volume distribution, but with a different chain packing theory at the molecular level (*19-21*).

All the theories previously discussed assumed semicrystalline chain packing for the polymer chains at the molecular level (*22*). The presence of small bundles of chains, which are parallel to each other, was experimentally shown using X-ray diffraction techniques (*15*). This parallel alignment of small polymer chain segments should not be confused with the regular chain packing in most crystalline or solid material. The molecular scale packing in these bundles of chain segments was further assumed to have a coordination number of four.

The model by Cohen and Turnbull assumes that four neighboring chains form a cage with a large enough free volume, within the cage, to accommodate many penetrant gas molecules

(*12,23*). The gas transport is then explained in terms of density fluctuations causing an opening in the cage, leading to the displacement of the molecules into another cage. The repetition of this procedure then leads to transport of the gas through the membrane.

The model proposed by DiBenedetto and Paul describes the transport of gas molecules to be parallel to the polymer chains (*19*). The gas molecule is assumed to be trapped in the bundle under equilibrium. During a thermal fluctuation the expansion of the chains near the molecule leads to a creation of cylindrical passage, thereby allowing the gas molecule to make a diffusional jump to the other end of this passage. With the closing of the passage, the gas molecule is at a new position under thermal equilibrium. On the macroscopic scale, this movement coincides with a small displacement of the gas molecule along the chain length. These random displacements result in the diffusion of the gas molecule through the membrane.

Pace and Datyner (*24*) incorporated the two variations of gas transport through the bundle of polymer chains to develop an elaborate theory which combined the parallel and perpendicular motion of gas molecules. This theory considered the case of a molecule moving along the polymer chain bundles and being stopped only by chain entanglements or a crystallite. In order to explain further motion of the gas molecule, it was proposed that the molecule then jumps into the adjacent bundles, similar to what Cohen and Turnbull had proposed. The jumping of molecules in between bundles was considered to be the rate controlling step, with the diffusion along the bundle being three times faster than the perpendicular jump of the molecule. This transport behavior was then mathematically expressed in terms of polymer density, cohesive energy density, Lennard Jones energy, and distance parameters. The minimum energy requirements for the parallel diffusional jump and the perpendicular jump were shown to be dependent on the penetrant diameter, the interchain stiffness, and the interchain cohesion.

The previously discussed descriptions for explaining the gas transport through glassy polymers are conceptually valid, but lack direct empirical evidence. Without experimental data, any theory concerning the gas transport process through glassy polymers can not be certain. Therefore, for all practical purposes, phenomenological models are used to describe the observed gas permeation process. These models are classified by either gas sorption or diffusion. Forthcoming discussions have been limited to gas sorption and diffusion in glassy polymers.

Sorption

The permeation behavior in glassy polymers has been modeled with respect to the diffusion–solution model. The failure of Henry's law to explain the higher sorption capability in glassy polymers is explained in terms of the presence of two or more modes for sorption. The concept of two or more modes for sorption of penetrants was initially presented by Matthes, in 1944, to study water sorption in cellulose (*7*). The first attempt to explain solubility of small molecules in glassy polymers, using this model, was presented by Meares in 1954. The mechanism was then modeled in its final form by Barrer, Michaels, and Vieth as the dual sorption model. The dual sorption model assumes that a polymer consists of a continuous chain matrix, along with microvoids (holes), frozen in the matrix. These microvoids, present in discrete as well as continuous domains, are caused by the non-equilibrium thermodynamic state of glassy polymers. The dual sorption mechanism modeled by equation (33) is then defined in terms of Henry's law of solubility (dissolution in continuous chain matrix) and Langmuir-type of sorption (sorption in microvoids). The basic assumptions during modeling are: (*23*)

1) The two modes occur simultaneously.
2) The two modes are always in equilibrium.
3) The penetrants sorbed under Langmuir mode are completely immobilized.
4) Diffusion occurs only in the dissolved mode.
5) The diffusion coefficient is independent of concentration.

The gas concentration in the polymer, for an applied pressure (p) is given as:

$$C = C_D + C_H = k_D p + \frac{C'_H \, bp}{(1 + bp)} \tag{33}$$

where C is the gas concentration, C_D is the gas concentration by normal dissolution, C_H is the gas concentration by hole filling, k_D is the Henry's law of dissolution constant, C'_H is the hole saturation constant, b is the hole affinity constant, and p is the gas pressure.

As local equilibrium is assumed between the C_D and C_H, the total concentration is expressed in terms of simply the normal dissolution concentration C_D.

$$C = C_D + \frac{KC_D}{(1+\alpha C_D)} \tag{34}$$

where

$$\alpha = \frac{b}{k_D} \text{ and} \tag{34.1}$$

$$K = \frac{C'_H\, b}{k_D} \tag{34.2}$$

The two parameters, b and C'_H, in the Langmuir isotherm are explained conceptually as the affinity of the gas molecules to get sorbed in holes (parameter b), and the total concentration of these holes in that polymer (parameter C'_H). The affinity parameter is described as the ratio of rate constants for sorption and desorption of gas molecules in the polymer. In the case of $bp<<1$, the gas solubility in glassy polymers is proportional to the applied gas pressure as modeled by Henry's law, whereas, for $bp>>1$, the sorption isotherm deviates from linearity by a constant value C'_H. Acceptance of this model is based on the agreement between the experimental results and theoretical predictions, along with the simple conceptual description of the process (*6,25-27*). The existence of Langmuir microvoids has been experimentally proven by NMR spectroscopy study on CO_2 sorption in polycarbonate (*28*).

Although the dual sorption model provides a conceptual reference for studying gas sorption in glassy polymers, it fails to correlate the sorption parameters to known properties of the polymer and the gas (*29*). Also, the presence of only two distinct modes is an oversimplification when considering the presence of sorption site size distribution. A more recent study has attempted to take into account these issues with partial success under some restriction (*30*). These restrictions include low sorption levels and an assumed spherical geometry of the molecule. However, these new developments are based on a novel combination of the lattice fluid model to explain Henry's mode sorption and a Gaussian distribution for microvoid sizes for Langmuir sorption sites. A statistical approach is then used to calculate the

fraction of free volume occupied by the gas at a given pressure, thereby estimating the gas solubility in the polymer (*31*).

Other models and explanations are presented in literature regarding gas sorption in glassy polymers. The gas-polymer matrix model by Raucher and Sefcid is based on the changes in polymer properties due to gas-polymer interactions (*32,33*). The sorbed gases are stated to interact with polymer chains, which alters the cooperative motions of the polymer chains, thereby leading to gas transport through the matrix. The model proposes a single sorption site with no physical insight given for the sorption process. The sorption isotherm expression does not provide a clear relationship between the material parameters and physical properties of gas-polymer system. It also is unable to describe mixed gas transport through polymers. Models based on lattice fluid models have also been proposed to predict sorption behavior. The Flory-Huggins lattice model and the Sanchez-Lacombe lattice fluid model are two examples of lattice fluid models. Unfortunately, these models are unable to describe the overall sorption behavior of different gas-polymer systems, under a wide range of environmental conditions.

Diffusion

The diffusion of gas molecules through glassy membranes is based on Fick's law of diffusion. When complete immobilization of the Langmuir mode sorbed gas molecules is assumed, the permeation flux equation is given as: (*34*)

$$J = -D_D\left(\frac{\partial C_D}{\partial x}\right) \tag{35}$$

where D_D is the diffusion coefficient for the Henry's law mode sorbed gas molecules. Paul (1969) presented a simple solution, where Fick's second law of diffusion was represented as:

$$-\frac{\partial J}{\partial x} = D_D\left(\frac{\partial^2 C_D}{\partial x^2}\right) = \frac{\partial}{\partial t}\left(C_D + C_H\right) \tag{36}$$

Petropoulos (*35*) suggested that the Langmuir mode adsorbed molecules could have mobility and complete immobilization was unlikely. The mobility in the Langmuir mode was

incorporated into the model by Petropoulos in terms of a dual mode transport model (*36-38*). The model was based on the chemical potential gradient as the driving force instead of the concentration and the unsteady state diffusion equation of Fick's second law, equation (37).

$$\frac{\partial C}{\partial t} = \frac{\partial}{\partial x}\left[\frac{1}{RT}\left(D_{T1}\cdot C_D + D_{T2}\cdot C_H\right)\frac{\partial \mu}{\partial x}\right] \tag{37}$$

where D_{TI} is the thermodynamic diffusion coefficient for the Henry's law mode sorbed species, D_{T2} is the thermodynamic diffusion coefficient for Langmuir species, μ is the chemical potential of the penetrant, R is the universal gas constant, and T is the absolute temperature.

Paul and Koros (*39*) presented the first partial immobilization model based on concentration gradient. The proposed modifications to the Fick's law of diffusion, defined in equation (35), was accomplished by introducing a new diffusion coefficient D_H for the mobility of the Langmuir mode species. The total permeation flux is then given as: (*39*)

$$J = -D_D\left(\frac{\partial C_D}{\partial x}\right) - D_H\left(\frac{\partial C_H}{\partial x}\right). \tag{38}$$

In equation (38), both diffusion coefficients are assumed to be concentration independent, with D_D generally much larger than D_H. To simplify the involved calculations, the factor F is introduced and defined as the ratio of the diffusion coefficient of the Langmuir mode and Henry's mode sorbed gas. The expression for the permeation flux and the permeability coefficient is then given as: (*39*)

$$J = -D_D\left[1 + F\left(\frac{\partial C_H}{\partial C_D}\right)\right]\cdot\left(\frac{\partial C_D}{\partial x}\right) \tag{39}$$

where

$$F = \frac{D_D}{D_H} \tag{39.1}$$

Barrer (*40*) proposed a dual transport based model incorporated with the partial immobilization at the molecular level. Barrer described the existence of four kinds of unit diffusion steps. Molecules sorbed by Henry's law (dissolved molecules) or those sorbed in the Langmuir mode (sorbed in holes) are denoted as *D* and *H*, respectively. Diffusion steps are defined as the various possibilities for a *D* or *H* molecule to jump into either another *D* or *H* site. These jumps can be represented as: (*40*)

(1) $D \rightarrow D$

(2) $H \rightarrow H$

(3) $D \rightarrow H$

(4) $H \rightarrow D$

To illustrate these jumps, the first case would imply, a dissolved gas molecule jumping into another site for dissolved molecule with associated diffusivity given as D_{DD}. The second case describes a sorbed molecule within a voidage jumping into another voidage with associated an associated diffusivity as D_{HH}. Cases three and four describe jump motions between Henry's law and Langmuir mode sites. Expressions are derived for each diffusional step in terms of jump frequency, distance per jump, associated diffusivities, vibration frequency, and the activation energy for a jump. The overall permeation flux was given as: (*40*)

$$J = J_{DD} + J_{HD} + J_{DH} + J_{HH} = \\ -\left[D_{DD} + D_{DH}\left(1-\theta'\right)\right]\cdot\frac{dC_D}{dx} - \left[D_{HH} + D_{DH} + D_{DH}\cdot\frac{C_D}{C_{sat}}\right]\cdot\frac{dC_H}{dx} \qquad (40)$$

where θ' is the fraction of total holes occupied by any molecule at any instant and is defined as:

$$\theta' = \frac{C_H}{C_{sat}} \qquad (40.1)$$

The final permeation expression for dual mode transport in terms of four diffusion jumps is then derived as: (*40*)

$$P = k_D \cdot D_{DD} + \frac{C'_H \, b\left(D_{HH} + D_{HD}\right) - k_D \cdot D_{DH}}{1 + bp} + 2k_D \cdot D_{DH} \cdot \frac{\ln\left(1 + bp\right)}{bp} \tag{41}$$

Barrer (*40*) used non-linear regression techniques to solve for the diffusion coefficients. Comparing this approach with the dual transport model, the relationship between the four unit diffusional jumps and the two coefficients are then given as:

$$D_D = D_{DD} + D_{DH} \cdot \left(1 - \theta\right) \tag{42}$$

and

$$D_H = D_{HH} + D_{HD} + D_{DH} \cdot \left(\frac{C_D}{C_{sat}}\right) \tag{43}$$

Thus, coefficient D_D denotes the relative frequency averaged appropriately for $D \rightarrow D$ and $D \rightarrow H$ jumps, which also holds true for D_H with respect to the $H \rightarrow H$ and $H \rightarrow D$ jumps (*40*).

Conclusions

In conclusion, the excellent agreement between the experimental data and the theoretical explanations presented by the dual mode sorption model makes this the most accepted model by most researchers to explain gas sorption in glassy polymers (*6,23,25,26,41-43*). The simplicity of the three parameter mathematical formulation and its applicability to most systems is another contributing factor to its wide use. This model has also been used in predicting the synergistic effects of gases on mixed gas transport (*44*). The reverse procedure of predicting sorption behavior by using sorption parameters, derived from permeability studies, has confirmed the validity of the model (*45*). However, the model fails to address the diffusional coupling effects on mixed gas transport through glassy polymers.

Gas Permeation in Crystalline Polymers

Crystalline polymers are comprised of uniform rigid chain packing. The crystal structure lacks both the sorption sites as well as the mobility of the chains to allow high mass transfer of gas molecules. Therefore, the gas transport through crystalline polymers is generally studied within the context of barrier properties (*46*). Crystalline and semi-crystalline materials are commercially important for food and beverage packaging.

Semi-crystalline Polymers

Sorption in Semi-crystalline Polymers

Semi-crystalline polymers have discrete sections of rigid chain packing on a macroscopic scale. These highly ordered sections hinder the dissolution of small gas molecules. Semi-crystalline polymers are discussed as materials consisting of two phases, namely the impermeable crystalline phase and the permeable amorphous matrix. Initial investigations revealed that the gas solubility is directly related to the crystallinity of the polymers. Bitter (1984) describes experiments which confirm the two phase model for a rubber amorphous phase. The solubility is then represented as: (*47*)

$$S = S_a \cdot \Phi_a \tag{44}$$

where, S_a is the solubility coefficient for pure amorphous polymer, and ϕ_a is the amorphous volume fraction.

Later investigation showed negative deviations from the simple two phase model (*48*). The behavior was explained in terms of the presence of unstable crystal structure which had higher density than the average density and was impermeable to gas. As the amorphous volume fraction was calculated based on average density measurements, these low density crystallites were assumed to cause the deviation. The potential for using gas sorption experiments for studying the change in the density of amorphous polymers is still being explored.

Diffusion in Semi-crystalline Polymers

The diffusion process in semi-crystalline polymers is studied in terms of a spatial

distribution of the impermeable crystalline phase and the permeable amorphous phase, which are cross-linked by tie chains (*48*). These tie chains cause reduced mobility for the chains in the amorphous phase. The gas permeate flux through a semi-crystalline polymer is given as: (*48*)

$$J = \alpha \cdot \left(\frac{D_a}{\tau} \right) \cdot \frac{\partial C}{\partial x} \tag{45}$$

where: D_a is the diffusivity of gas for a completely amorphous polymer, α is the cross sectional area available to transport, τ is the tortuosity factor accounting for the hindrance to the gas molecules due to the presence of the crystalline phase.

The cross-linking effects are accounted for by introducing a factor β, which accounts for the high activation energy required for gas diffusion through such polymers. The diffusion coefficient can be defined as: (*48*)

$$D = \left(\frac{D_a}{\tau \cdot \beta} \right). \tag{46}$$

The idea of chain immobilization due to cross-linking effects is of low significance for the polymeric system with high backbone rigidity. Attempts have been made to correlate the chain immobilization parameter to the penetrant diameter and the amorphous volume fraction. The tortuosity factor can be correlated to the volume fraction by a power law relationship. Annealing a semi-crystalline polymer leads to a 50% reduction in the tortuosity factor. This finding was used to explain the formation of semi-permeable gaps in formed large crystallites (*48*).

Liquid Crystalline Polymers

Liquid crystalline polymers (LCP) recently gained popularity because of their excellent mechanical properties achieved from conventional melt processing methods. This class of polymers are also referred to as mesomorphic, meaning middle form. These polymers have received considerable attention due to their highly oriented morphology resulting in ultra high

strength (*49*). The unique packing arrangement of rigid monomer and flexible spacers results in a different mechanism of gas transport through these materials (*46,50*).

Sorption in Liquid Crystalline Polymers

Compared with semi-crystalline polymers, the gas transport through LCPs is generally very low. The increased barrier properties of LCPs is often explained by two prominent theories. One theory suggests that the presence of a liquid crystalline order retards gas transport by acting as a three dimensional impermeable crystal structure. The second theory suggests that the efficient packing of chains in the liquid crystalline phase is ultimately responsible for hindering gas transport. These theories have been questioned by numerous researcher because they are unable to explain the increase in diffusion coefficients observed for LCP polymers (*46*).

Diffusion in Liquid Crystalline Polymers

Gas diffusion through LCPs is not well defined. Only speculative explanations on gas diffusion for these materials are found in literature and no standard observations for gas transport through LCPs exist. The only definitive statement that can be made concerning gas transport through LCPs is that their permeability is generally lower then a similar semi-crystalline polymer.

Effects of Environmental Conditions on Polymer Permeability

Temperature Effects on Permeability

Sorption

The thermal effects on solubility and diffusion show opposite trends. Generally, for gas adsorption, solubility decreases with increases in temperature due to the condensability of the peneatrant at lower temperatures. The solubility dependence with temperature is typically written in terms of the van't Hoff relationship (*26*).

$$S = S_0 \cdot \exp\left(-\frac{\Delta H_s}{R \cdot T}\right) \tag{47}$$

where S_0 is a constant and ΔH_s is the partial molar enthalpy of sorption. The solubility in thermodynamic terms is a two step process (*26*). The first step involves the condensation of the gas molecule in a polymer, followed by creation of a molecular scale gap for accommodating the gas molecule. These individual steps contribute to the total enthalpy of sorption and are mathematically represented as: (*26*)

$$\Delta H_s = \Delta H_{condensation} + \Delta H_{mixing} . \tag{48}$$

For low molecular weight super critical gases, low condensability causes the mixing step to control the sorption property of a polymer. For weak interactions between the gas molecule and the polymer, the change in enthalpy of mixing is positive. This leads to an increase in solubility with an increase in temperature. For the case of condensable gases and vapors, the enthalpy change for condensation is negative and dominant, thereby showing decreasing solubility with increasing temperature (*26*).

Diffusion

Temperature dependence on gas diffusion is expressed in terms of an Arrhenius type relationship, as movement of gas molecules through a membrane is considered a thermally activated process (*15*). Mathematically, the temperature dependence of diffusion is given as: (*15*)

$$D = D_0 \cdot \exp\left(\frac{E_D}{R \cdot T}\right) \tag{49}$$

where D_0 is the pre exponential factor and E_D is the activation energy of diffusion. Studies on the thermal effects during gas transport have shown that the activation energy term is dependent on the size of the penetrant and not on its mass (*12,15*). Diffusion is the most temperature sensitive transport parameter, in comparison to solubility and permeability (*42*). Combining the temperature dependence equations for the diffusion and sorption coefficients, the temperature effect on gas permeability is given as: (*15*)

$$P = P_0 \cdot \exp\left(\frac{E_P}{R \cdot T}\right) \tag{50}$$

where E_P is the activation energy of permeation and is an algebraic sum of E_D and ΔH_s. In general, permeability increases with increasing temperature. However, there are exceptions, especially near the glass transition temperature of the polymer, where opposite trends have been observed. Experiments with CO_2 permeation through a polyimide membrane showed decreased permeability with increased temperature (*51*). The same behavior was also observed for butane permeation through polyimide polymers. These observations were explained in terms of pressure effects on the polymer under isothermal operating conditions. The high stress caused by the applied gas pressure was stated to cause a transition in the polymer from a rubbery state to a glassy state.

Specifically in glassy polymers, all three gas transport parameters decrease with increasing temperature. Some exceptions are observed at high temperatures where low solubility cause more errors in the fitting of the dual mode sorption curve (*42*). Koros (*25*) reports that highly open, rigid chain polymers exhibited lower temperature dependence on gas transport properties than corresponding flexible chain polymers.

Pressure and Concentration Effects on Permeability

Gas transport is modeled according to ideal operating conditions. However, large deviations are observed between the theoretical predictions and the experimental gas transport parameter values for non-ideal environmental conditions, particularly at elevated pressures. The affect of pressure and therefore the gas concentration in the membrane is a major challenge in effective modeling of the gas transport process. Typical effects of gas pressure on permeability is shown in Figure 3 (*42*). Response A is for the ideal case where diffusion and solubility are assumed to be independent of gas pressure. This type of behavior is observed for the case of supercritical gas permeation in amorphous polymers. Response B is characteristic of a gas plasticization effect on the polymer and is observed during organic vapor permeation in rubbery polymers. Response C corresponds to the case of highly soluble gases in glassy polymers. Response D is a combination of responses (B) and (C) and is observed in the case of permeation of organic vapors or plasticizing gas, such as CO_2, in glassy polymers.

The deviations from the ideal behavior (response A) are caused by the affect of pressure on either solubility or the diffusion coefficient (*52*). With the diffusion coefficient dependent on gas concentration, the permeation flux is expressed: (*52*)

$$P = -D(C)\cdot\left(\frac{\partial C/\partial x}{\Delta p/h}\right) \tag{51}$$

As the permeability coefficient is constant for a given upstream and downstream pressure, the product of the diffusion coefficient and ($\partial C/\partial x$) should be constant. Equation (51) can be expressed in an alternative form upon application of a mathematical manipulation technique, separation of variables (*52*).

$$\frac{p}{h}\int_0^h dx = \int_{C_1}^{C_a} D(C)\cdot\frac{dC}{dp}\cdot dp \tag{52}$$

For downstream pressure ($C_1=0$), the final permeability equation is derived as: (*52*)

$$P = \left[\int_0^{C_2} D(C)\cdot\frac{dC}{C_2}\right]\cdot\left[\frac{C_2}{p_2}\right] = D\cdot S \tag{53}$$

The diffusion coefficient describes the kinetics of the transport phenomena whereas the gas solubility is governed by the thermodynamic interaction between the penetrant and the membrane material. The integrated formulation of the permeation process, equation (52), equates both the polymer-penetrant dynamics (kinetic factor), as well as the polymer-penetrant interactions (thermodynamic factor).

Sorption

The thermodynamic factor (dC/dp) in equation (56) is modeled in the form of a sorption isotherm. The sorption behavior for any gas/vapor-polymer system is classified into four types of isotherms, Figure 4 (*42,53*). Response A represents an ideal gas-polymer system without

specific interactions. This linear variation is represented by Henry's law of solubility. Response B corresponds to a homogenous swelling of rubbery polymers with compatible penetrants. Similar behavior is also observed with complex polar and hydrogen bonding penetrants dissolved in non-polar rubbery polymers. This behavior is generally valid wherever the penetrant molecules form clusters because of strong interaction with each other. Response C represents the dual mode sorption isotherm and is observed in gas sorption in glassy polymers. Response D shows an inflection point and is observed with highly soluble penetrants in glassy polymers. The Flory-Huggins solubility equation is used for estimating the solubility of organic vapors at high pressure in polymers (*26,53*).

Diffusion

The concentration dependence of the diffusion coefficient is generally studied indirectly as direct experimental measurements are hard to perform. Indirect measurement can be made by experimentally measuring the pressure dependence on solubility and permeability of a gas in a polymer. Based on these separate observations, the pressure dependence on diffusion is deduced as the ratio of permeability and solubility. Using a similar approach that is used for studying pressure dependence on gas solubility and permeability, the four typical isotherms observed for diffusion are shown in Figure 5.

Response A occurs when polymers are exposed to organic vapors or hydrophilic polymers exposed to water. Response B is observed for plasticizing penetrants present at very low concentration, thereby giving a linear response. Response C is commonly observed for glassy polymers and well described by the dual mode sorption model. The expression relating the effective diffusion coefficient, in terms of ideal diffusion coefficient for the dissolved penetrant, equation (36), is given as: (*42*)

$$D_{eff}(C) = D_D \cdot \left\{ \frac{1 + \left[F \cdot K \Big/ (1 + \alpha \cdot C_D) \right]^2}{1 + \left[K \Big/ (1 + \alpha \cdot C_D) \right]^2} \right\} \tag{54}$$

where

$$F = \frac{D_D}{D_H} \tag{54.1}$$

$$K = \frac{C'_H \cdot b}{k_D} \tag{54.2.}$$

Response D is characteristic of clustering penetrants. For example, molecules with hydrogen bonding capabilities show and increase in effective diameter of the gas molecules at high gas pressures. This then leads to a decrease in the effective diffusion coefficient. Alternatively, the chemical interactions between the polymer and the penetrant have shown peculiar responses with increasing penetrant pressure. The effect of CO_2 is shown to induce plasticization in various polymers at different penetrant pressures (*11,43,50,54-62*).

Experimental Determination of Permeation Rate

The permeation rate of a diffusant through a sheet or membrane can be obtained by either the steady-state diffusion or time-lag technique. Both of these techniques require well-defined conditions of surface concentration. The surface concentration will remain constant if it is in equilibrium with a constant-concentration source of diffusant. The diffusant can be in contact with the sheet or membrane in a solution, or as a constant pressure of gas or vapor (*8*). Experimental methods used to estimate gas transport properties through polymers, can be divided into two categories: (1) integral permeation method; and (2) differential permeation method.

Integral Permeation Method

Integral permeation is performed by allowing the penetrant to permeate through a initially degassed polymer membrane, and accumulate in an evacuated chamber. The rise in pressure at constant volume or the increase in volume at constant pressure is then monitored with respect to time. The barometric technique is used to monitor the pressure rise in a known downstream volume and is the most commonly used technique to measure the permeability of pure gases, condensable vapors and gas vapor mixtures. This method is still the focus for development and various modifications have been made since its conception. The improved design of membrane

cells to allow constant feed concentration of gas mixtures has been the most dramatic improvement. Instruments used for monitoring the pressure rise have changed from a simple manometer to sophisticated strain gauges and capacitance type pressure transducers (*11*).

The ASTM standard barometric method for measuring gas transmission rates and permeabilities is designated D1434-82 (*63*). The ASTM barometric method utilizes a Dow gas transmission cell, Figure 6 (*63*). The membrane is supported with filter paper, and sealed with an "O" ring. An open-end mercury manometer is used to measure the pressure in the receiving chamber.

The ASTM standard volumetric method for measuring gas transmission rates and permeabilities is also designated D1434-82 (*63*). The ASTM volumetric method utilizes a Linde permeation cell, Figure 7 (*63*). This procedure operates by imposing a positive pressures on both sides of a membrane supported by filter paper. The permeating gas displaces a slug of fluid in a calibrated capillary tube. After steady state is achieved, the slug velocity is measured using a cathetometer and a stopwatch. Permeation rate is calculated based on the velocity of the liquid slug and cross-sectional area of the tube. It is recommended that the permeation cell be contained with a temperature controlled liquid bath. The volumetric method is commonly used for measurements of relatively high permeation rates and is less sensitive then the barometric approach.

Gravimetric techniques are commonly used to measure water vapor transmission, but can also be applied to other gases. A gravimetric permeation system is comprised of a desiccant sealed in a container partially or entirely enclosed by the test material. The container is exposed to the penetrant atmosphere, and its weight is monitored with time (*11*). The gravimetric method is only recommended for test materials exhibiting high steady-state permeation rates.

A host of analytical techniques and devices have been developed to determine penetrant concentrations in the receiving volumes of closed permeation cells. They include labeling of penetrant molecules and determining penetrant concentration by: radiometric methods, infrared absorption spectroscopy, electrolytic decomposition, refractive index measurement, mass spectroscopy, and sensory analysis (*11*).

Differential Permeation Method

Differential permeation methods, also known as open receiving volume permeation experiments, include an apparatus that dynamically measures penetrant concentration. The two basic techniques employed in this type of permeation experiments are the continuous flow cell and the weighing cup method (*11*). The continuous flow cell technique is the more commonly used technique among the two. A typical continuous flow permeation apparatus, Figure 8, introduces a penetrant into a chamber on one side of a membrane, with the permeating gases passing through the membrane into a flowing gas stream (*11*). The rate is analyzed by measuring the concentration of the effluent gas and multiplying it with the gas flow rate. This method has several advantages over integral closed-volume methods. The ability to measure the instantaneous rate of permeation rather than a total penetrant mass permits the attainment of a true steady state and offers a significant improvement over closed-volume systems. Another advantage to the differential continuous flow approach is that equal pressure can be maintained on both sides of a membrane. This diminishes the imposed pressures on the membrane seal and provides motion of the gas on one or both sides of the membrane. Dynamic gas flow greatly decreases the effects of gas phase mass transfer resistance. The design of the membrane cell should include a large membrane surface to volume ratio. This is especially important when measuring low permeation rates in order to satisfy the initial and boundary conditions of the model.

The measurement of gas concentration can be performed by numerous analytical techniques. Several of these techniques include: hygrometers, electrolytic cells, and gas chromatographs equipped with every conceivable detector (*11,64-71*). Automated dynamic cell systems are available commercially. For example, the MAS 2000 Organic Vapor Permeation Test System (Testing Machines Inc., Amityville, NY) allows for the continuous collection and measurement of the permeation rate of organic vapors through a polymer membrane, from the initial time zero to steady-state conditions. This apparatus incorporates a flame ionization detector (FID) with precise temperature and flow rate controls and is interfaced to a computer system (*72*).

The weighing cup technique is used for measuring steady state permeation rates for saturated vapors for relatively high permeable membranes (*11*). A typical setup includes a container filled with liquid and covered by a membrane. The weight loss of the liquid with

respect to time is monitored to calculate the permeation rate. This method is the least accurate of the experimental method discussed in review.

Experimental Determination of Sorption and Desorption

Gravimetric Determination of Sorption and Desorption

Gravimetry is the technique most often used to determine the sorption and/or solubility coefficients of gas or vapor/polymer systems (*73*). A gravimetric sorption experiment generally includes a sample put into contact with an atmosphere with a controlled gas concentration until equilibrium is reached. The uptake is calculated by the weight gained by the sample. Gravimetry replicates real packaging conditions better then any other mass-sorption technique, but also is the most time consuming technique. A complete isotherm commonly takes longer then one month to obtain. In addition, it is difficult to obtain data at very low sorbate activities by gravimetry (*74*).

Various instruments have been used for gravimetry experiments. The first and most common device, known as a McBain balance, Figure 9, is based on the extension of a calibrated spring due to gas sorption (*11*). In a typical system, a McBain spring system consists of a water-jacketed glass chamber attached to a vacuum pump for polymer degassing and sorbate removal. The chamber temperature is controlled by the water bath. A small polymer sample (25-50 mg) is loaded into a cylindrical quartz pan suspended from a sensitive helical quartz spring in the chamber. Before beginning sorption experiments, the polymer sample is exposed to vacuum until no further spring displacement is observed in order to remove any previously sorbed air gases from the polymer. The polymer sample is then exposed to a sorbate at fixed pressure, and the spring position relative to a fixed reference rod hanging in the chamber is recorded (*11*). The McBain balance apparatus is frequently used to obtain sorption isotherms for water and organic vapors in contact with food grade polymers (*75-77*).

Gravimetry experiments have been automated to include an electrobalance that digitally records sorption uptake. The exposure chamber for the polymer is similar to the one described in the McBain spring apparatus. The two systems differ in that the measuring device for sorption uptake for the electroblance system is a precise electrobalance connected to a computer acquisition program via a computer interface. Common electrobalances used for electrogravimetry experiments are Cahn or Sartorius microbalances demonstrating sensitivity =

10^{-7} g and precision = 10^{-6} g. Solubility and diffusion coefficients for gases in polymers are routinely determined by electrogravimetry (*73,78-83*).

Barometric Determination of Sorption and Desorption

The barometric method is generally used for high pressure sorption measurements. This technique is based on the introduction of known amount of gas into an evacuated volume containing the polymer sample. The method requires an accurate knowledge of the system volume, as transducers or manometers are used to monitor the decrease in pressure due to gas sorption. A typical barometric sorption apparatus consists of two chambers of known volume, Figure 10. The reservoir chamber, connected to the pressure transducer, is filled with a known amount of gas and then introduced into the sorption chamber, containing the degassed polymer sample. With prior knowledge of the amount of gas present and the two chamber volumes, the pressure decay is then related to the transport parameters (*11*). The barometric technique is a versatile technique for measuring sorption properties of different polymers. This method is being modified to measure sorption characteristics at very high temperatures (>200°C) and pressure (>30 atm) using better materials for their construction and sophisticated measuring tools (*84*).

Volumetric Determination of Sorption and Desorption

Another technique used for sorption measurements is the volumetric technique. This technique employs the measurement of the volume change in the chamber at constant pressure to calculate the gas sorption. This technique is not used commonly as it requires accurate feed back control for maintaining constant pressure. The volumetric sorption apparatus most often described in literature is the Rosen volumetric sorption apparatus, Figure 11. This apparatus uses a manometer to measure the difference between a preset pressure, and the pressure in the sorption chamber. Mercury is used to compensate for the amount of gas sorbed by the sample. The loss of mercury measured through a manometer tube can be monitored to estimate the volume change.

Inverse Gas Chromatography Determination of Sorption and Desorption

Introduction

Inverse gas chromatography (IGC) is an excellent technique to study the adsorption of organic vapors by polymers (*85-91*). IGC measures substrate-adsorbate interactions, but does not have the ability to make conclusions or quantify bulk sorption. However, IGC gives a good approximation for total mass-sorption for crystalline and semi-crystalline polymers where bulk sorption is significantly restricted (*92*). Experiments comparing the sorption in different substrates obtained by IGC and gravimetry have shown that differences are below 10% (*93-95*).

Unlike many mass-sorption experiments, IGC allows the measurement of adsorption data for very low vapor concentrations (Henry's law concentration region), where only substrate-adsorbate interactions are important. Another advantage to IGC is that it allows the determination of a complete adsorption isotherm in a relatively short time (*92,96*). In addition to studying the adsorption of organic vapors by polymers, IGC is used to determine thermal transitions and characterization of surface properties and crystallinity of polymers (*97*). In fact, IGC is presently the only experimental technique that yields thermodynamic information on polymer blends with relative ease (*98*).

Determination of Sorption by IGC

Kiselev and Yashin Sorption Model

"The fundamental parameter measured in IGC is the retention volume (V_R), which is the volume of carrier gas required to elute a solute vapor from the column. This parameter describes the equilibrium partitioning of the solute vapor between the stationary and mobile phases" (*92*). Martin (*99*) described that surface interaction and bulk diffusion contribute independently to V_R by the following equation:

$$V_R = K_S A + K_B V_B \tag{55}$$

where V_R is the measured net retention volume of the probe corrected for pressure drop along the column and temperature, A is the total surface area of the stationary phase, V_B is the total volume of the stationary phase, and K_S and K_B are the surface and bulk partition coefficients, respectively.

Retention volume is calculated using: (*92*)

$$V_R = (t_r - t_0) \cdot f\left(\frac{T_C}{T_R} \cdot \frac{3}{2} \cdot \frac{(P_{in}/P_{out})^2 - 1}{(P_{in}/P_{out})^3 - 1}\right) \tag{56}$$

where t_r is the retention time of the probe, t_0 is the retention time of a non-reacting species, f is the measured flow rate, T_C and T_R are the column and room temperature, and P_{in} and P_{out} are the column inlet and outlet pressures, respectively. Equation (56) reduces to: (*92*)

$$V_R = K_S A \tag{57}$$

for gas-solid chromatography systems, where the stationary phase polymer is below its glass transition temperature (T_g) and when surface adsorption is the predominant retention mechanism. Equation (57) neglects diffusion of the sorbate probe into the bulk of the stationary phase. If A is known, the surface coefficient, K_S, can easily be calculated from equation (57). K_S values are significant because they characterize the adsorbate-adsorbent equilibrium (*92*).

Kiselev and Yashin (*90*) derived a method for the calculating adsorption isotherms from the shape of a single gas chromatographic peak. Equation (58) calculates the uptake (a) of an adsorbed species by the stationary phase directly from a chromatogram.

$$a = \frac{A_{ads} \cdot m_a}{a_{cal} \cdot m_p} \tag{58}$$

where A_{ads} is the area framed by elution time of a non-retained probe, posterior peak profile, base line and peak height, Figure 12, a_{cal} is the calibration peak area on the recorder chart corresponding to an injection of m_s grams of probe, m_s is the mass of the probe, and m_p is the mass of adsorbent (*74,92*).

The partial pressure of the sorbate (p_s) entering the gas chromatographic detector may be related to the experimental chromatogram by: (*92*)

$$p_s = \frac{M_s \cdot R \cdot T_C \cdot cs \cdot h}{M_s \cdot \mu \cdot A_{ads}} \tag{59}$$

where M_s is the molecular weight of the sorbate, R is the universal gas constant, T is the column temperature, cs is the recorder chart speed, h is the chromatographic peak maximum, and μ is the carrier gas flow rate corrected to account for pressure drop along the length of the column.

Equation (59) is more often expressed in terms of sorbate activity, p_s/p_s^v, for IGC experiments examining the scalping of aroma components into polymers used for food packaging. The activity of the sorbate (p_s/p_s^v) can be related to the experimental chromatogram by: (*74*)

$$\frac{p_s}{p_s^v} = \frac{n \cdot R \cdot T_C \cdot cs \cdot h}{P_s^v \cdot \mu \cdot A_{cal}} \tag{60}$$

where n is the number of injected sorbate moles.

In order to calculate the partial pressure of the sorbate, p_s, entering the gas chromatographic detector by equation (59) or the activity of the sorbate, p_s/p_s^v, by equation (60), one must first calculate the corrected carrier gas flow rate, μ. The corrected carrier gas flow rate can be calculated from the measured flow rate, f, using the James-Martin compressibility factor: (*74*)

$$\mu = \frac{f \cdot \mathrm{T}}{\mathrm{T_e}} \cdot \frac{\left[\left(P_{in}/P_e\right)^3 - 1\right]}{\left[\left(P_{in}/P_e\right)^2 - 1\right]} \tag{61}$$

where T_e is the room temperature, P_e is the environmental pressure of the room, and P_{in} is the pressure at the head of the column.

Adsorption isotherms (sorbate uptake versus the partial pressure of the sorbate entering the chromatographic detector), Figure 13, or sorption isotherms (sorbate uptake versus sorbate activity), Figure 14, are commonly constructed in order to compare substrate-adsorbate interactions for different sorbate-adsorbate systems. Partition coefficients, K_s, are calculated using equation (57) from the experimental retention volume, V_R, and the total area of the

adsorbent determined empirically or by using the Brunnauer-Emmitt-Teller (BET) approach (*92,100*). Alternatively, one can indirectly obtain the solubility coefficient, *S*, for a sorbate from a sorption isotherm graph. Henry's law defines the solubility coefficient of a sorbate in a polymeric system as: (*74*)

$$S = \frac{c_p^s}{p_v} \tag{62}$$

where c_p^s is the concentration of sorbate in the polymer and p_v is its partial vapor pressure. For linear sorption isotherms, the solubility coefficient can be obtained from the slope of the sorption isotherm, dw/da_s, and the partial pressure of the sorbate at saturation, p_v^s, by the following equation: (*74*)

$$S = \frac{\left(dw / da_s\right)}{p_v^s}. \tag{63}$$

Values of *S* are extensively used to provide data on vapor sorption in polymers used for food packaging applications (*101*).

Khan and Pawlisch Sorption Models

Khan developed a method to model the dispersion of a solute slug flowing through a capillary column (*102*). This model can be applied to IGC experiments where retention time measurements can be used to determine thermodynamic data such as Henry constants, infinite dilution activity coefficients, and Flory-Huggins interaction parameters. In addition, the shape of the chromatographic peak allows one to obtain information related to the transport phenomena in the column (*102*).

Three factors have been identified to contribute to band broadening in packed columns; eddy diffusion (the *A*-term), longitudinal diffusion (the *B*-term), and mass transfer in the stationary phase (the *C*-term). The van Deemter model expresses broadening in terms of plate height, *H*, as a function of the linear gas velocity, μ. In its simple form, the van Deemter model is: (*103*)

$$H = A + \frac{B}{\mu} + C \cdot \mu \tag{64}$$

In capillary columns, eddy diffusion is negligible and the *A*-term is dropped from equation (64).

Plate height can be determined from the eluted peak by the relation: (*102*)

$$H = L \cdot \frac{\sigma_t^2}{t_r^2} \tag{65}$$

where L is the column length, σ^2_t is the peak variance, and t_r is the retention time.

In equation (64), the term B / μ becomes infinitely small and negligible at high flow rates. Therefore, a plot of H versus μ produces a linear plot with a slope of C. Once C is determined, one can calculate the probe diffusion coefficient in the stationary phase by the following equation: (*102*)

$$C = \left(\frac{8}{\pi^2}\right) \cdot \left(\frac{\tau^2}{D_p}\right) \cdot \left(\frac{K}{\varepsilon}\right) \cdot \left(\frac{1+K}{\varepsilon}\right)^{-2} \tag{66}$$

where D_p is the diffusion coefficient of the stationary phase, τ is the film thickness, K is the partition coefficient, and ε is the ratio of the stationary-phase volume to the gas-phase volume.

Equation (66) is only valid when; (1) the entire mass transfer resistance within the column is due to diffusion in the stationary phase; (2) stationary phase support is spherical and uniform; (3) film thickness is constant and uniform; and (4) instrumental and thermodynamic contributions are negligible (*102*). The liquid film distribution in packed columns is not uniform. Therefore, the constant $8/\pi^2$ in equation (66) must be replaced by an experimentally determined geometric factor, *q'* and the film thickness, τ, at its deepest point. The *q'* can be obtained by eluting a probe whose D is already known. Unfortunately, the method just described for packed columns is an indirect method for measuring D and thus, only relative D of solutes can be

determined. No information about the column geometry can be made and the composition of the chromatographic column becomes a non-controllable variable (*102*).

It is possible to obtain a uniform distribution of the stationary phase on the tube wall of a capillary column. This makes it easier to model the dispersion of a solute flowing through a capillary column. Khan developed a model for describing this solute dispersion in a capillary column. According to Khan's model, there are four kinetic phenomena that contribute to peak broadening: (1) radial diffusion of the solute in the stationary phase; (2) radial diffusion of the solute in the mobile phase; (3) axial diffusion of the solute in the mobile phase; and (4) interfacial mass transfer resistance. The basic equations of Khan's model are:

$$\mu_1 = \left(1 + \frac{2 \cdot K \cdot \tau}{R'}\right) \cdot t_0 \tag{67}$$

$$\begin{aligned} \mu_2^* &= \frac{\int_0^\infty (t - \mu_1)^2 \cdot C(t) dt}{\int_0^\infty C(t) dt} \\ &= \left[\frac{4 \cdot \tau^3 \cdot K}{3 \cdot R' \cdot D_p} \cdot \frac{1}{t_0} + \frac{2 \cdot D_g \cdot (1 + K')^2}{L^2} \cdot t_0 + \frac{\left(1 + 6K' + 11K'^2\right) \cdot R'^2}{24 \cdot D_g} + \frac{4 \cdot K \cdot \tau^2}{R' \cdot K_d} \cdot \frac{1}{t_0}\right] \cdot t_0^2 \end{aligned} \tag{68}$$

$$\mu_2^* = \left[a \cdot \frac{1}{t_0} + b \cdot t_0 + c + d \cdot \frac{1}{t_0}\right] \cdot t_0^2 \tag{69}$$

where $K' = (2K\tau/R')$; t_0 is the residence time of the carrier gas; μ_1 is the mean retention time (first statistical moment); μ_2^* is the variance of the distribution (second central statistical moment); $C(t)$ is the solute concentration in the gas phase at time t; D_g is the gas-phase diffusion coefficient; R' is the column inner radius; and K_d is the interfacial desorption rate coefficient.

Equations (68) and (69) demonstrate that terms that contribute to peak broadening include: (1) carrier flow rate, $1/t_c$; column geometry for the stationary phase; and the probe diffusion coefficient in the stationary and mobile phases (*102*).

Pawlisch et al. (*104*) simplified Khan's model for systems in which the stationary phase is a polymer. The interfacial resistance and radial diffusion are negligible in polymeric stationary phases. According to Pawlisch and his coworkers equation (69) can be simplified to:

$$\mu_*^2 = \left[\frac{4 \cdot \tau^3 \cdot K}{3 \cdot R \cdot t_c \cdot D_p} + \frac{2 \cdot D_g \cdot t_c}{L^2} \cdot \left(1 + 2 \cdot \tau \cdot \frac{K}{R} \right)^2 \right] \cdot t_c^2 \qquad (70)$$

For capillary columns with thick films, greater then 1.2 μm in most instances, the second term in equation (70) is negligible and D_p can be calculated upon determination of film thickness, inner radius, and retention time of a non-adsorbed probe: (*102*)

$$\mu_2^* = \frac{4 \cdot \tau^3 \cdot K}{3 \cdot R \cdot D_p} \cdot t_c \qquad (71)$$

Thermodynamics of Adsorption

In addition to accurately determining adsorption isotherms for molecular probes, IGC has the ability to make conclusion concerning the thermodynamics of adsorption of infinite dilution. For example, the standard Gibbs free energy (ΔG_s^0) for the isothermal transfer of 1 mol of adsorbate from the reference standard adsorption state, defined by the gas pressure, $p_{s'}$, to an adsorbate state, defined by its equilibrium partial pressure, p_s, is given by: (*92*)

$$\Delta G_s^0 = RT \ln\left(\frac{p_s}{p_{s'}}\right) \tag{72}$$

De Boer (*105*) defines adsorbate standard state as the surface pressure π_s (π_s is a measure of the reduction in the surface free energy of a solid as a result of the adsorption of a vapor at an equilibrium pressure p_s), such that the average separation of the adsorbed molecule, in an assumed ideal two dimesional gas, is identical to the average separation in the gas phase at 1 atm and 0°. The equilibrium partial pressure of the sorbate, p_s, is calculated by equation (59).

Experimental Parameterers for IGC

Introduction

As was previously discussed, the key parameter in IGC experiments is the retention volume. Therefore, the experimental variables contributing to the calculation of retention volume must precisely be measured. These variables include: pressures, times, weights, and flow rates. In particular, proper preparation and characterization of the chromatographic column is the most essential aspect in obtaining good IGC results (*106*).

Preparation of Packed Columns

Packed columns are the most common chromatographic columns used in IGC studies. Packed columns are suitable for a wide range of investigations, including low molecular weight materials, homo- and copolymers, blends, and block copolymers (*84,107-111*). In IGC studies where packed columns are used, the stationary phase generally consists of a non-interacting solid support that is uniformly coated with a thin film of a test polymer. The two most common supports used for IGC packed columns are Chromasorb W, manufactured by Johns Mansville, and 60/80 mesh sized glass beads. Successful loading ranges for Chromasorb W and glass beads have been reported to be 4 to 13% and 0.5% by weight, respectively (*106*).

The stationary phase is commonly applied by dissolving the polymer is a suitable solvent and filtering the mixture. A quantity of the inert support is weighed in order to achieve a desired ratio of inert support to stationary phase once the solvent is removed. The inert support and filtered polymer solution are placed into a hedgehog flask. A hedgehog flask is a pear shaped

flask with vigreux fingers extending to its interior. Coating is achieved by slow evaporation of the solvent at reduced pressure using a rotary evaporator. This method provides complete and uniform coverage of the stationary phase onto the support (*106*).

Alternatively, one can apply the stationary phase by a soaking method developed by Al-Saigh and Munk (*98*). This method more accurately assesses the amount of polymer on the support then does the rotary evaporator coating method. The soaking method dissolves the stationary phase polymer in a suitable solvent and pours this mixture over the support, which is piled uniformly on a watch glass. Care is taken to wet the pile as much as possible without letting the solution touch the surface of the dish, either around or under the pile. The solvent is allowed to evaporate and the pile is thoroughly mixed. This procedure is repeated until all of the solution is applied and the flask is rinsed with solvent several times. Typically, 10-20 applications are needed.

Both methods require complete removal of solvent. Bolvari et al. (*106*) recommends drying the coated support in a vacuum oven for 48 hours at a temperature just below the glass transition temperature (T_g) of the stationary phase. The packing should then be sifted through a mesh sieve to ensure even particle sizes.

Several researchers have chosen not to coat an inert support with stationary phase material, but instead directly pack a chromatographic column with stationary phase in the form of discs, strips, threads, or powder. Katz and Gray (*89*) mechanically produced small discs from cellophane film which was then used to pack a chromatographic column to be used for IGC experiments. Anhang and Gray (*85*) reported a similar packing technique to the one described by Katz and Gray for poly(ethylene terephthalate) PET. Gavara et al. (*74*) packed chromatographic columns with linear low density poly(ethylene) (LLDPE) and PET film strips which were then used to study aroma scalping by IGC. Direct stationary phase packing in the form of thin fibers is another packing technique (*86,88,106*). Fiber columns are the hardest columns in which to prepare and are often reserved for determination of thermodynamic surface properties.

Inverse gas chromatography water sorption experiments for non-synthetic macromolecules have recently been performed. Demertzis et al. (*94*) studied the water sorption behavior of pectins by packing chromatographic columns with powdered pectins and using IGC

methods to calculate sorption isotherms for water. Il et al. (*93*) packed chromatographic columns with powdered gliadin and used IGC to characterize its water sorption.

The packed chromatographic column is usually stainless steel in composition, has a ¼ inch outside diameter (o.d.), and is 1 to 2 meters in length. The column is packed with the aid of a mechanical vibrator and vacuum pump. The column is precisely weighed before and after packing in order to determine the total weight of the stationary phase in the column. The column is conditioned by purging it with helium for 30 minutes at ambient temperature. The temperature is then raised to 10 degrees above the T_g or the crystalline melt temperature (T_m), whichever is highest for the stationary phase, and is held at that temperature of 12 hours. This conditioning further removes any residual solvent and solvent-induced morphologies present in the polymer when this is applicable (*106*).

The weight of the stationary phase can be determined by ashing, using a thermogravimetric analysis system (TGA) when a coating technique is used. A small amount of coated support, 5 to 10 mg, is loaded onto a TGA sample pan and the TGA oven temperature is raised to 550°C in an oxygen atmosphere. Measurements must be made on both the coated and non-coated support to correct for the weight loss of the inert solid support (*106*).

Preparation of Capillary Columns

IGC experiments have also been performed using open tubular capillary column, but not to the extent at which packed columns have been used. Capillary columns are generally 5 to 50 m in length and have an internal diameter of 0.1 to 0.53 mm. The inside wall of the tubing is coated with a stationary phase film ranging from 0.1 μm to 3.0 μm in thickness. A major advantage of capillary columns is that many chromatographic plates are obtainable. Capillary columns have been manufactured using stainless steel, glass, and fused silica. Fused silica columns are preferred because of flexibility and inertness (*103*).

The goal when preparing capillary columns for IGC experiments is to apply the stationary phase uniformly throughout the column. Two methods are generally used when coating capillary columns. These techniques are known as the dynamic and static method. The dynamic method requires 10 mL of dilute polymer solution (6 to 10 wt%) to be placed in a reservoir and pushed through the column with nitrogen at reduced pressure (0.5 atm). A continuous nitrogen flow is applied to the column in order to dry the polymer to the tubes inner

walls. A 10 mL portion of the coating solution is put through the column as many times as is necessary to obtain the desired film thickness (*106*).

The static technique for coating capillary columns is the method more often used by researchers because of its ability to determine the film thickness more accurately then by the dynamic method. The concentration of the coating solution that is used to fill the column ultimately determines the column's film thickness. The column is filled with a coating solution and then carefully sealed at one end. The column is then placed in a water bath and connected to a vacuum via the open end until complete evaporation of the coating solution is achieved. Capillary columns are conditioned by purging them with helium and increasing the temperature by 0.5°C / min until complete removal of the solvent (*102*).

When the static technique is used to coat the interior wall of the chromatographic column, the final film thickness can readily be determined by the concentration of the coating solution by the following equation: (*102*)

$$\tau = \frac{R \cdot p}{200} \tag{73}$$

where τ is the film thickness (microns); R is the column inner radius (microns); and p is the volume percent of the polymer in solution (*102*). The average inner diameter of the capillary column is measured experimentally by weighing a portion of the column, filling it with mercury, weighing the column again, and finally measuring its length. This procedure is extremely accurate for obtaining the average inner diameter of capillary columns (*102*).

Determination of Stationary Phase Surface Area for Packed Columns

The surface area of a coated inert support can be determined empirically by nitrogen adsorption using a Micrometrics Pulse Chemisorb Model 2700 apparatus (Noricross, GA). Gas mixtures of various concentrations of nitrogen in helium can be passed through a sample of the coated support, and then cooled to -196°C. Adsorption or desorption of nitrogen can then be determined from changes in nitrogen/helium composition. Nitrogen/helium concentration is measured by a thermal conductivity detector (TCD) (*92*).

In addition, surface areas can be calculated from adsorption isotherm data using the BET

theory (*100,112*). If p_s^v is the saturation vapor pressure of the probe and m_0 is the amount of the probe adsorbed on the surface at monolayer coverage, the BET equation can be written:

$$\frac{p_s / p_s^v}{a\left(1 - p_s / p_s^v\right)} = \frac{1}{m_0 C} + \frac{C-1}{m_0 C} \cdot p_s / p_s^v \tag{74}$$

where C is a constant for a given probe/adsorbent system and is related to the heat of adsorption. A plot of $p_s/p_s^v a(1- p_s/p_s^v)$ versus p_s/p_s^v is linear with slope equal to $(C-1/m_0C)$. Thus, m_0 and C are determined. The monolayer value can then be used to determine the surface area, S', per gram of adsorbent using: (*92*)

$$S' = \frac{1}{m_s} \cdot N \cdot A_a \cdot m_0 \tag{75}$$

where m_s is the mass of the probe, N is Avogadro's number and A_a is the area of the probe molecule. Molecular area (A_a) can be estimated from the density of the liquid probe, assuming that the arrangement of the probe molecules on the surface is the same as on a plane surface placed with the bulk of the liquid (*107*). Based on this assumption, A_a can be expressed: (*92*)

$$A_a = 1.091\left(\frac{M_s}{\rho N}\right)^{2/3} \cdot 10^{14} \tag{76}$$

where M_s is the molecular weight of the probe, ρ_s is the density of the probe and 1.091 is the packing factor. Values of m_0, S', and A_a, are determined by means of equations (74), (75), and (76). The BET approach and the nitrogen adsorption method show excellent agreement when calculating stationary phase surface area. Kontominas et al. (*92*) reports a 99.5% agreement between the methods when determining the surface area of polystyrene coated glass beads.

Determination of Stationary Phase Surface Area for Capillary Columns

The surface area of the stationary phase in capillary columns can be determined either empirically by the cryogenic nitrogen approach or theoretically by the BET approach. Surface

area per gram of adsorbent, *S'*, can be calculated using equations (74) and (75). Molecular area, A_a, is calculated upon determination of film thickness by equation (73) and multiplying this value by the length of the column.

Fourier Transform Infrared Spectroscopy (FTIR) Attenuated Total Reflection (ATR Determination of Sorption and Desorption

The use of i*n-situ* FTIR-ATR spectroscopy to study diffusion in polymer systems is unique in that this technique measures diffusivity in a diffusion-out mode rather than using a mass-sorption (diffusion-in) methodology (*113*). This technique more accurately measures the external migration of additives in a polymer matrix to an outside environment rather then the internal migration of additives from an outside environment into a polymer matrix, the former simulating the actual process in commercial films more accurately.

The diffusion of a polymeric additive can be measured through the construction of a mathematical model, which is then solved analytically. As an example, the diffusion coefficient can be deduced for a sorption experiment in which M_t/M_∞ is plotted as a function of $(t/l^2)^{1/2}$. The main disadvantage of this approach is the establishment of M_∞, which requires lengthy experimental times. Experimental error can also be compounded in mass-sorption experiments by repeated handling of film, the use of a film which is too thin, and evaporation of diffusant from the polymeric surface during the weighing (*113*).

Passiniemi (*114*) constructed a model for the determination of *D* for solvents and gases in polymers. This model states that the diffusion coefficient can be calculated by determining the differences of measured quantity, ΔM, as a function of *t*. The uniqueness of this model is that differences of measured quantity, ΔM, can be measured by any concentration-dependent quantity, including spectroscopic absorption. Additionally, one does not need to know specifically the dependence of the measured dependence of the measured quantity on the concentration of the diffusing species, nor does one need to measure the equilibrium state of the system. The model is given as: (*114*)

$$\ln\left[\Delta M(t)\right] = \ln\left[M(t+\Delta t) - M(t)\right] = -\lambda_1 Dt + K \qquad (77)$$

where ΔM is measured by IR absorbance, Δt is a fixed time interval between measurements, and K is a constant. The diffusion coefficient can be obtained from the slope of a plot of $\ln[\Delta A(t)]$ versus t.

The diffusivity of erucamide, a polymeric additive used in poly(ethylene) (PE) and poly(propylene) (PP) films to improve surface-slip or anti-blocking properties, has been determined by *in-situ* FTIR-ATR spectroscopy (*113*). Recently, *in-situ* FTIR-ATR spectroscopy has been used to measure diffusion coefficients of low molecular weight volatiles by mass-sorption techniques. The diffusion coefficient for water vapor in poly(acrylonitrile) (PAN) and PET has accurately been determined by *in-situ* FTIR-ATR (*115,116*).

Miscellaneous Techniques for Determination of Sorption and Desorption

Other techniques have been developed for sorption studies, but these studies are usually either too costly or restricted to specific systems (*11*). King (*117*) developed a piezoelectric sorption device, which includes a crystal coated with a known mass of polymer. The crystal has a resonant frequency, which changes as the gas is sorbed into the polymer. This method is well suited for gas sorption measurements under a wide range of operating temperatures and pressures. This technique has been used to study the sorption of ethylene by polyethylene (*118,119*).

Assink (*120*) used pulsed nuclear magnetic resonance spectrometry to study the sorption of ammonia in polystyrene. This seminal study helped in confirming one of the basic assumptions in the dual mode sorption theory, which is the assumption of an equilibrium between the gas sorbed by Henry's mode and the gas sorbed by Langmuir mode.

References

(1) Quijada-Garrido, I.; Barrales-Rienda, J. M.; Frutos, G. Diffusion of erucamide (13-*cis*-docosenamide) in isotatic polypropylene. *Macromolecules* **1996**, *29*, 7164-7176.

(2) Földes, E. Transport of small molecules in polyolefins. II. Diffusion and solubility of Irganox 1076 in ethylene polymers. *J. Appl. Polym. Sci.* **1993**, *48*, 1905-1913.

(3) Klein, J.; Briscoe, B. J. Diffusion of long molecules through solid polyethylene. II. Measurement and results. *J. Polym. Sci., Polym. Phys. Ed.* **1977**, *15*, 2065-2074.

(4) Rawls, A. Diffusion of an erucamide slip additive in linear low-density polyethylene film. M.S., Clemson University, 1997.

(5) Schlotter, N. E.; Furlan, P. Y. A review of small molecule diffusion in polyolefins. *Polymer* **1992**, *33*, 3323-3342.

(6) Stern, S. A. Polymers for gas separations: the next decade. *J. Membr. Sci.* **1994**, *94*, 1-65.

(7) Stannett, V. The transport of gases in synthetic polymeric membranes - An historic perspective. *J. Membr. Sci.* **1978**, *3*, 97-115.

(8) Crank, J. Methods of measurement. In *Diffusion in Polymers*; J. Crank and G. S. Park, Eds.; Academic Press: New York, 1968; pp 1-39.

(9) Frisch, H. L. The time lag in diffusion. *J. Phys. Chem.* **1957**, *61*, 93-95.

(10) Vahdat, N.; Sullivan, V. D. Estimation of permeation rate of chemical through elastometric materials. *J. Appl. Polym. Sci.* **2000**, *79*, 1265-1272.

(11) Felder, R. M.; Huvard, G. S. Permeation, diffusion, and sorption of gases and vapors. In *Methods of Experimental Physics: Polymers*; R. A. Fava, Ed.; Academic Press: New York, 1980; pp 315-377.

(12) Crank, J.; Park, G. S. Methods of measurement. In *The Mathematics of Diffusion*; J. Crank, Ed.; Oxford University Press: London, 1975; pp 1-39.

(13) Miltz, J. *Food Product-Package Compatibility Proceedings, East Lansing, MI*; Technomic Publishing, p 30-37.

(14) Alexopoulos, J. B.; Barrie, J. A.; Machin, D. The time lag for the diffusion of gas mixtures. *Polymer* **1969**, *10*, 265-269.

(15) Kesting, R. E.; Fritzsche, A. K. *Polymeric gas separation membranes*; John Wiley & Sons, Inc.: New York, 1993.

(16) Tant, M. R.; Wilkes, G. L. An overview of the nonequilibrium behavior of polymer glasses. *Polym. Eng. Sci.* **1981**, *21*, 874-895.

(17) Stern, S. A.; Fang, S. M.; Frisch, H. L. Effect of pressure on gas permeability coefficients. New application of "free volume" theory. *J. Polym. Sci. A-2, Polym. Phys.* **1972**, *10*, 201-219.

(18) Fang, S. M.; Stern, S. A.; Frisch, H. L. Free volume model of permeation of gas and liquid mixtures through polymeric membranes. *Chem. Eng. Sci.* **1975**, *30*, 773-780.

(19) DiBenedetto, A. T.; Paul, D. R. Interpretation of gaseous diffusion through polymers using fluctuation theory. *J. Polym. Sci. Pt. A* **1964**, *2*, 1001-1015.

(20) DiBenedetto, A. T. Molecular properties of amorphous high polymers. II. Interpretation of gaseous diffusion through polymers. *J. Polym. Sci. Pt. A* **1963**, *1*, 3477-3487.

(21) DiBenedetto, A. T. Molecular properties of amorphous high polymers. I. A cell theory for amorphous high polymers. *J. Polym. Sci. Pt. A* **1963**, *1*, 3459-3476.

(22) Vrentas, J. S.; Duda, J. L. Diffusion of small molecules in amorphous polymers. *Macromolecules* **1976**, *9*, 785-790.

(23) Vieth, W. R. *Membrane Systems: Analysis and Design*; Hanser Publishers: New York, 1988.

(24) Pace, R. J.; Datyner, A. Statistical mechanical model for diffusion of simple penetrants in polymers. I. Theory. *J. Polym. Sci., Polym. Phys. Ed.* **1979**, *17*, 437-451.

(25) Koros, W. J.; Fleming, G. K. Membrane-based gas separation. *J. Membr. Sci.* **1993**, *83*, 1-80.

(26) Ghosal, K.; Freeman, B. D. Gas separation using polymer membranes: An overview. *Polym. Adv. Technol.* **1994**, *5*, 673-697.

(27) Robeson, L. M. Correlation of separation factor versus permeability for polymeric membranes. *J. Membr. Sci.* **1991**, *62*, 165-185.

(28) Cain, E. J.; Wen, W.-Y.; Jones, A. A.; Inglefield, P. T.; Cauley, B. J.; Bendler, J. T. A dual-mode interpretation of spin relaxation for $^{13}CO_2$ sorbed in polycarbonate. *J. Polym. Sci.: Part B: Polym. Phys.* **1991**, *29*, 1009-1020.

(29) Banerjee, T.; Lipscomb, G. G. Mixed gas sorption in elastic solids. *J. Membr. Sci.* **1994**, *96*, 241-258.

(30) Jordan, S. S.; Koros, W. J. A free volume distribution model of gas sorption and dilation in glassy polymers. *Macromolecules* **1995**, *28*, 2228-2235.

(31) Kirchheim, R. Sorption and partial molar volume of small molecules in glassy polymers. *Macromolecules* **1992**, *25*, 6952-6960.

(32) Raucher, D.; Sefcik, M. D. Gas transport and cooperative main-chain motions in glassy polymers. In *Industrial Gas Separations*; T. E. Whyte; C. M. Yon and E. H. Wagener, Eds.; American Chemical Society: Washington, DC, 1983; pp 89-110.

(33) Raucher, D.; Sefcik, M. D. Gas-polymer-matrix model. In *Industrial Gas Separation*; T. E. Whyte; C. M. Yon and E. H. Wagener, Eds.; American Chemical Society: Washington, DC, 1983; pp 111-124.

(34) Paul, D. R. Effect of immobilizing adsorption on the diffusion time lag. *J. Polym. Sci. A-2, Polym. Phys.* **1969**, *7*, 1811-1818.

(35) Petropoulos, J. H. Quantitative analysis of gaseous diffusion in glassy polymers. *J. Polym. Sci. A-2, Polym. Phys.* **1970**, *8*, 1797-1801.

(36) Petropoulos, J. H. Membranes with non-homogenous sorption and transport properties. *Adv. Polym. Sci.* **1985**, *64*, 93-142.

(37) Petropoulos, J. H. On the dual mode gas transport model for glassy polymers. *J. Polym. Sci.: Part B: Polym. Phys.* **1988**, *26*, 1009-1020.

(38) Petropoulos, J. H. A generalized, topologically consistent dual mode transport model for glassy polymer-gas systems. *J. Polym. Sci.: Part B: Polym. Phys.* **1989**, *27*, 603-620.

(39) Paul, D. R.; Koros, W. J. Effect of partial immobilizing sorption on permeability and the diffusion time lag. *J. Polym. Sci., Polym. Phys. Ed.* **1976**, *14*, 675-685.

(40) Barrer, R. M. Diffusivities in glassy polymers for the dual mode sorption model. *J. Membr. Sci.* **1984**, *18*, 25-35.

(41) Vieth, W. R. *Diffusion In and Through Polymers: Principles and Applications*; Hansen Publishers: New York, 1991.

(42) Koros, W. J.; Chern, R. T. Separation of gaseous mixtures using polymer membranes. In *Handbook of Separation Process Technology*; R. W. Rousseau, Ed.; John Wiley & Sons, Inc.: New York, 1987; pp 862-953.

(43) Costello, L. M.; Koros, W. J. Comparison of pure and mixed gas CO_2 and CH_4 permeabilities in polycarbonate: Effect of temperature. *Ind. Eng. Chem. Res.* **1993**, *32*, 2277-2280.

(44) Koros, W. J.; Chan, A. H.; Paul, D. R. Sorption and transport of various gases in polycarbonate. *J. Membr. Sci.* **1977**, *2*, 165-190.

(45) Subramanian, S.; Heydweiller, J. C.; Stern, S. A. Dual mode sorption kinetics of gasses in glassy polymers. *J. Polym. Sci.: Part B: Polym. Phys.* **1989**, *27*, 1209-1220.

(46) Weinkauf, D. H.; Paul, D. R. Effects of structure order on barrier properties. In *Barrier Polymers and Structures*; W. J. Koros, Ed.; American Chemical Society: Washington, DC, 1990; pp 60-91.

(47) Bitter, J. G. A. Effect of crystallinity and swelling on the permeability and selectivity of polymer membranes. *Desalination* **1984**, *51*, 19-35.

(48) Vieth, W. R.; Wuerth, W. F. Transport properties and their correlation with the morphology of thermally conditioned polypropylene. *J. Appl. Polym. Sci.* **1969**, *13*, 685-712.

(49) Chiou, J. S.; Paul, D. R. Gas transport in a thermotropic liquid crystalline polyester. *J. Polym. Sci.* **1987**, *25*, 1699-1707.

(50) Kamiyu, Y.; Hirose, T.; Mizoguchi, K.; Terada, K. Sorptive dilation of poly(vinylbenzoate) and poly(vinyl butyral) by carbon dioxide. *J. Polym. Sci.: Part B: Polym. Phys.* **1988**, *26*, 1409-1424.

(51) Costello, L. M.; Koros, W. J. Thermally stable polyimide isomers for membrane-based gas separations at elevated temperatures. *J. Polym. Sci.: Part B: Polym. Phys.* **1995**, *33*, 135-146.

(52) Frisch, H. L. Pressure dependence of diffusion in polymers. *J. Elastoplastics* **1970**, *2*, 130-132.

(53) Kamiyu, Y.; Hirose, T.; Mizoguchi, K.; Naito, Y. Gravimetric study of high pressure sorption of gases in polymers. *J. Polym. Sci.: Part B: Polym. Phys.* **1986**, *24*, 1525-1539.

(54) Kamiyu, Y.; Hirose, T.; Mizoguchi, K.; Terada, K. Sorptive dilation of polysulfone and poly(ethylene terephthalate) films by high pressure carbon dioxide. *J. Polym. Sci.: Part B: Polym. Phys.* **1988**, *26*, 159-177.

(55) Koros, W. J.; Paul, D. R. Carbon dioxide sorption in poly(ethylene terephthalate) above and below the glass transition. *J. Polym. Sci., Polym. Phys. Ed.* **1978**, *16*, 1947-1963.

(56) Wonders, A. G.; Paul, D. R. Effects of carbon dioxide exposure history on sorption and transport in polycarbonate. *J. Membr. Sci.* **1979**, *5*, 63-75.

(57) Toi, K.; Ito, T.; Ikemoto, I. Effect of aging and conditioning on the gas transport in poly(vinyl acetate). *J. Polym. Sci.: Part B: Polym. Lett.* **1985**, *23*, 525-529.

(58) Maeda, Y.; Paul, D. R. Effect of antiplasticization on gas sorption and transport. I. Polysulfone. *J. Polym. Sci.: Part B: Polym. Phys.* **1987**, *25*, 957-980.

(59) Maeda, Y.; Paul, D. R. Effect of antiplasticization on gas sorption and transport. II. Poly(phenylene oxide). *J. Polym. Sci.: Part B: Polym. Phys.* **1987**, *25*, 981-1003.

(60) Maeda, Y.; Paul, D. R. Effect of antiplasticization on gas sorption and transport. III. Free volume interpretation. *J. Polym. Sci.: Part B: Polym. Phys.* **1987**, *25*, 1005-1016.

(61) Kumazawa, H.; Wang, J. S.; Naito, K.; Messaoudi, B. Gas transport in polymer membrane at temperatures above and below glass transition point. *J. Appl. Polym. Sci.* **1994**, *51*, 1015-1020.

(62) Chern, R. T.; Koros, W. J.; Sanders, E. S.; Yui, R. "Second component" effects in sorption and permeation of gases in glassy polymers. *J. Membr. Sci.* **1983**, *15*, 157-169.

(63) American Society for Testing and Materials Standard test method for determining gas permeability characteristics of plastic film and sheeting. In *1998 Annual Book of ASTM Standards*;; Am. Soc. Test. Mater.: Philadelphia, PA, 1998; pp 1-12.

(64) Hernández-Muñoz, P.; Catalá, R.; Hernandez, R. J.; Gavara, R. Food aroma mass transport in metallocene ethylene-based copolymers for packaging applications. *J. Agric. Food Chem.* **1998**, *46*, 5238-5243.

(65) Zimmerman, C. M.; Singh, A.; Koros, W. J. Diffusion in gas separation membrane materials: a comparison and analysis of experimental characterization techniques. *J. Polym. Sci.: Part B: Polym. Phys.* **1998**, *36*, 1747-1755.

(66) Gavara, R.; Hernandez, R. J. The effect of water on the transport of oxygen through nylon-6 films. *J. Polym. Sci.: Part B: Polym. Phys.* **1994**, *32*, 2375-2382.

(67) Leufvén, A.; Stöllman, U. Polymer films as aroma barriers at different temperatures. *Lebensm. Unters. Forsch.* **1992**, *194*, 355-359.

(68) Paik, J. S. Comparison of sorption in orange flavor components by packaging films using the headspace technique. *J. Agric. Food Chem.* **1992**, *40*, 1822-1825.

(69) Schoene, K.; Steinhanses, J.; König, A. Determination of the solubility of vapours in polymers by automated headspace gas chromatography. *J. Chromatogr.* **1988**, *455*, 67-75.

(70) Kontominas, M. G. Determination of permeation rates of polymeric films to various organic vapors in relation to retention of flavor quality of packaged foodstuffs. *Sciences des aliments* **1985**, *5*, 321-329.

(71) Ziegel, K. D.; Frensdorff, H. K.; Blair, D. E. Measurement of hydrogen isotope transport in poly(vinyl fluoride) films by the permeation-rate method. *J. Polym. Sci. A-2, Polym. Phys.* **1969**, *7*, 809-819.

(72) Huang, S. J.; Giacin, J. R. Evaluating the effect of temperature and vapor concentration on the organic vapor barrier properties of polymer membranes by an isostatic procuedure. *J. Plastic Film Sheeting* **1998**, *14*, 308-333.

(73) Hernandez, R. J.; Gavara, R. Sorption and transport of water in nylon-6 films. *J. Polym. Sci.: Part B: Polym. Phys.* **1994**, *32*, 2367-2374.

(74) Gavara, R.; Catalá, R.; Hernández-Muñoz, P. Study of aroma scalping through thermosealable polymers used in food packaging by inverse gas chromatography. *Food Additives and Contaminants* **1997**, *14*, 609-616.

(75) McDowell, C. C.; Coker, D. T.; Freeman, B. D. An automated spring balance for kinetic gravimetric sorption of gases and vapors in polymers. *Rev. Sci. Instrum.* **1998**, *69*, 2510-2513.

(76) Ponangi, R.; Pintauro, P. N. Measurement and interpretation of equilibrium organic vapor sorption in polyurethane membranes. *J. Membr. Sci.* **1998**, *144*, 25-35.

(77) Serad, G. E.; Freeman, B. D.; Stewart, M. E.; Hill, A. J. Gas and vapor sorption and diffusion in poly(ethylene terephthalate). *Polymer* **2001**, *42*, 6929-6943.

(78) Barr, C. D.; Giacin, J. R.; Hernandez, R. J. A determination of solubility coefficient values determined by gravimetric and isotatic techniques. *Packag. Technol. Sci.* **2000**, *13*, 157-167.

(79) Hernandez-Muñoz, P.; Gavara, R.; Hernandez, R. J. Evaluation of solubility and diffusion coefficients in polymer film-vapor systems by sorption experiments. *J. Membr. Sci.* **1999**, *154*, 195-204.

(80) Jonquières, A.; Perrin, L.; Durand, A.; Arnold, S.; Lochon, P. Modelling of vapour sorption in polar materials: Comparison of Flory-Huggins and related models with the ENSIC mechanistic approach. *J. Membr. Sci.* **1998**, *147*, 59-71.

(81) Li, S.; Paik, J. S. Flavor sorption estimation by UNIFAC group contribution model. *Trans. ASAE* **1996**, *39*, 1013-1017.

(82) Roland, A. M.; Hotchkiss, J. H. Determination of flavor - Polymer interactions by vacuum-microgravimetric method. In *Food and Packaging Interactions II*; S. J. Risch and J. H. Hotchkiss, Eds.; American Chemical Society: Washington, DC, 1991; pp 149-160.

(83) Wong, B.; Zhang, Z.; Handa, Y. P. High-precision gravimetric technique for determining the solubility and diffusivity of gases in polymers. *J. Polym. Sci.: Part B: Polym. Phys.* **1998**, *36*, 2025-2032.

(84) Costello, L. M.; Koros, W. J. Temperature dependence of gas sorption and transport properties in polymers: Measurements and applications. *Ind. Eng. Chem. Res.* **1992**, *31*, 2708-2714.

(85) Anhang, J.; Gray, D. G. Surface characterization of poly(ethylene terephthalate) film by inverse gas chromatography. *J. Appl. Polym. Sci.* **1982**, *27*, 71-78.

(86) Chappell, P. J. C.; Williams, D. R. Determiniation of poly(*p*-phenylene terehthalamide) fiber surface cleanliness by inverse gas chromatogrpahy. *J. Colloid Interface Sci.* **1989**, *128*, 450-457.

(87) Demertzis, P. G.; Kontominas, M. G. Thermodynamic study of water sorption and water vapor diffusion in poly(vinylidene chloride) copolymers. In *Inverse Gas Chromatography. Characterization of Polymers and Other Materials*; D. R. Lloyd; T. C. Ward; H. P. Schreiber and C. C. Pizaña, Eds.; American Chemical Society: Washington, DC, 1989; pp 77-86.

(88) Gozdz, A. S.; Weigmann, H.-D. Surface characterization of intact fibers by inverse gas chromatography. *J. Appl. Polym. Sci.* **1984**, *29*, 3965-3979.

(89) Katz, S.; Gray, D. G. The adsorption of hydrocarbons on cellophane. *J. Colloid Interface Sci.* **1981**, *82*, 318-325.

(90) Kiselev, A.; Yashin, Y. I. *Gas-Adsorption Chromatography*; Plenum Press: New York, 1969.

(91) Shiyao, B.; Sourirajan, S.; Talbot, F. D. F.; Matsuura, T. Gas and vapor adsorption on polymeric materials by inverse gas chromatography. In *Inverse Gas Chromatography. Characterization of Polymers and Other Materials*; D. R. Lloyd; T. C. Ward; H. P. Schreiber and C. C. Pizaña, Eds.; American Chemical Society: Washington, DC, 1989; pp 59-76.

(92) Kontominas, M. G.; Gavara, R.; Giacin, J. R. The adsorption of hydrocarbons on polystyrene by inverse gas chromatography: infinite dilution concentration region. *European Polymer Journal* **1994**, *30*, 265-269.

(93) Il, B.; Daun, H.; Gilbert, S. G. Water sorption of gliadin. *J. Food Sci.* **1991**, *56*, 510-512, 531.

(94) Demertzis, P. G.; Riganakos, K. A.; Giannakakos, P. N.; Kontominas, M. G. Study of water sorption behaviour of pectins using a computerised elution gas chromatographic technique. *J. Sci. Food Agric.* **1991**, *54*, 421-428.

(95) Faridi, N.; Hadj-Romdhane, I.; Danner, R. P.; Duda, J. L. Diffusion and sorption in ethylene-propylene copolymers: comparison of experimental methods. *Ind. Eng. Chem. Res.* **1994**, *33*, 2483-2491.

(96) Etxeberria, A.; Etxabarren, C.; Iruin, J. J. Comparison between static (sorption) and dynamic (IGC) methods in the determination of interaction parameters in polymer/polymer blends. *Macromolecules* **2000**, *33*, 9115-9121.

(97) Vîlcu, R.; Leca, M. *Polymer Thermodynamics by Gas Chromatography*; Elsevier Science Publishers: New York, 1990.

(98) Al-Saigh, Z. Y.; Munk, P. Study of polymer-polymer interaction coefficients in polymer blends using inverse gas chromatography. *Macromolecules* **1984**, *17*, 803-809.

(99) Martin, R. L. Adsorption on the liquid phase in gas chromatography. *Anal. Chem.* **1961**, *33*, 347-352.

(100) Brunauer, S.; Emmitt, P. H.; Teller, E. Adsorption of gases in multimolecular layers. *J. Am. Chem. Soc.* **1938**, *60*, 309-319.

(101) Gavara, R.; Hernandez, R. J.; Giacin, J. R. Methods to determine partition coefficient of organic compounds in water/polystyrene systems. *J. Food Sci.* **1996**, *61*, 947-952.

(102) Bonifaci, L.; Carnelli, L.; Cori, L. Determination of infinite dilution diffusion and activity coefficients of solvents in polystyrene by inverse gas chromatography on a capillary column. *J. Appl. Polym. Sci.* **1994**, *51*, 1923-1930.

(103) McNair, H. M.; Miller, J. M. *Basic Gas Chromatography: Techniques in Analytical Chemistry*; John Wiley & Sons: New York, 1998.

(104) Pawlisch, C. A.; Macris, A.; Laurence, R. L. Solute diffusion in polymers. 1. The use of capillary column inverse gas chromatography. *Macromolecules* **1987**, *20*, 1564-1578.

(105) De Boer, J. H. *The Dynamic Character of Adsorption*, 2nd ed.; Oxfored University Press: London, 1968.

(106) Bolvari, A. E.; Ward, T. C.; Koning, P. A.; Sheehy, D. P. Experimental techniques for inverse gas chromatography. In *Inverse Gas Chromatography. Characterization of Polymers and Other Materials*; D. R. Lloyd; T. C. Ward; H. P. Schreiber and C. C. Pizaña, Eds.; American Chemical Society: Washington, DC, 1989; pp 12-19.

(107) Gray, D. G.; Guillet, J. E. A gas chromatographic method for the study of sorption on polymers. *Macromolecules* **1972**, *5*, 316-321.

(108) Gray, D. G.; Guillet, J. E. Studies of diffusion in polymers by gas chromatography. *Macromolecules* **1973**, *6*, 223-227.

(109) Kong, J. M.; Hawkes, S. J. Diffusion in uncrosslinked silicones. *Macromolecules* **1975**, *8*, 685-687.

(110) Braun, J. M.; Poos, S.; Guillet, J. E. Determination of diffusion coefficients of antioxidants in polyethylene by gas chromatography. *J. Polym. Sci.: Part B: Polym. Lett.* **1976**, *14*, 257-261.

(111) Ward, T. C.; Sheehy, D. P.; McGrath, J. E.; Davidson, T. F.; Riffle, J. S. Inverse gas chromatography studies of poly(dimethylsiloxane)-polycarbonate copolymers and blends. *Macromolecules* **1981**, *14*, 1791-1797.

(112) Brunauer, S. About some critics of the BET theory. *Langmuir* **1987**, *3*, 3-4.

(113) Gagliardi, C. A.; Muire, L. B.; Hirt, D. E. *Annual Technical Conference, Clemson University, Clemson, SC*; Vol. 57, p 2502-2506.

(114) Passiniem, P. General theory for determination of diffusion coefficients of solvents and gases in polymers. *Polymer* **1995**, *36*, 341-344.

(115) Fieldson, G. T.; Barbari, T. A. The use of FTIR-ATR spectroscopy to characterize penetrant diffusion in polymers. *Polymer* **1993**, *34*, 1146-1153.

(116) Sammon, C.; Everall, N.; Yarwood, J. The diffusion of water into PET followed by *in-situ* using FT-IR ATR. *Macromol. Symp.* **1997**, *119*, 189-196.

(117) King, W. H. Using quartz crystals as sorption detectors ... part 1. *Res. Dev.* **1969**, *20*, 28-34.

(118) Bonner, D. C.; Cheng, Y. L. A new method for determination of equilibrium sorption of gases by polymers at elevated temperatures and pressures. *J. Polym. Sci.: Part B: Polym. Lett.* **1975**, *13*, 259-264.

(119) Cheng, Y. L.; Bonner, D. C. Solubility of ethylene in liquid, low-density polyethylene to 69 atmospheres. *J. Polym. Sci., Polym. Phys. Ed.* **1977**, *15*, 593-603.

(120) Assink, R. A. Investigation of the dual mode sorption of ammonia in polystyrene by NMR. *J. Polym. Sci.: Part B: Polym. Lett.* **1975**, *13*, 1665-1673.

Chapter 4 Appendix

Figure 1. Schematic representation of gas transport through a polymer membrane *(42)*.

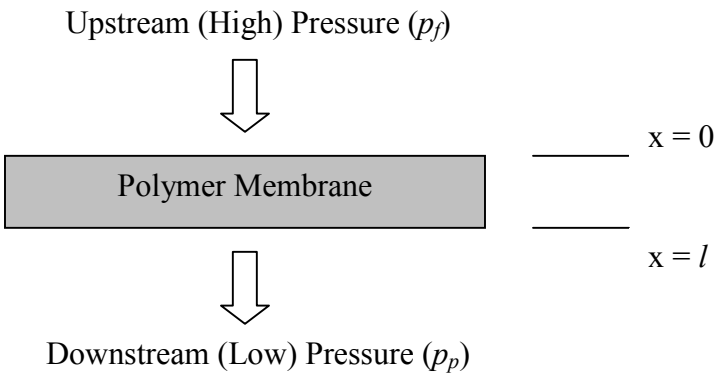

Figure 2. Sorption cycles for several transport mechanisms in a polymer. (a) Fickian diffusion, constant D; (b) Fickian diffusion, D increases with increasing C; (c) Fickian diffusion, D decreases with decreasing C; (d) anomalous or case II transport; (e) two-stage sorption *(11)*.

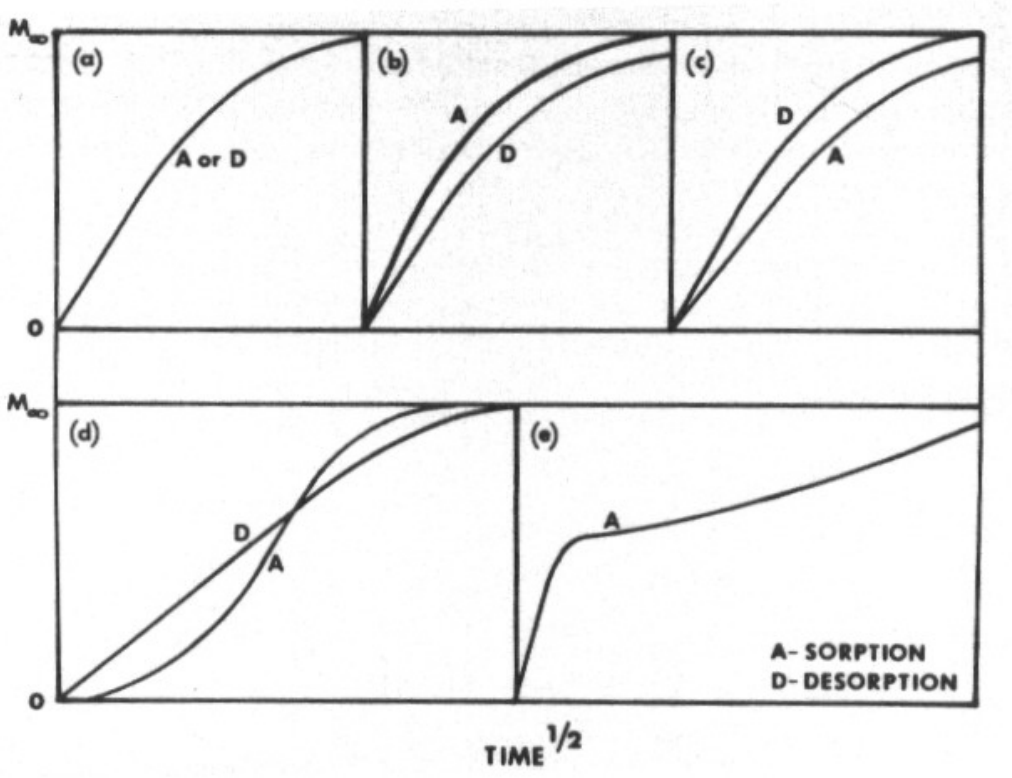

Figure 3. Forms of permeability dependence on gas concentration during gas transport through polymer membranes *(42)*.

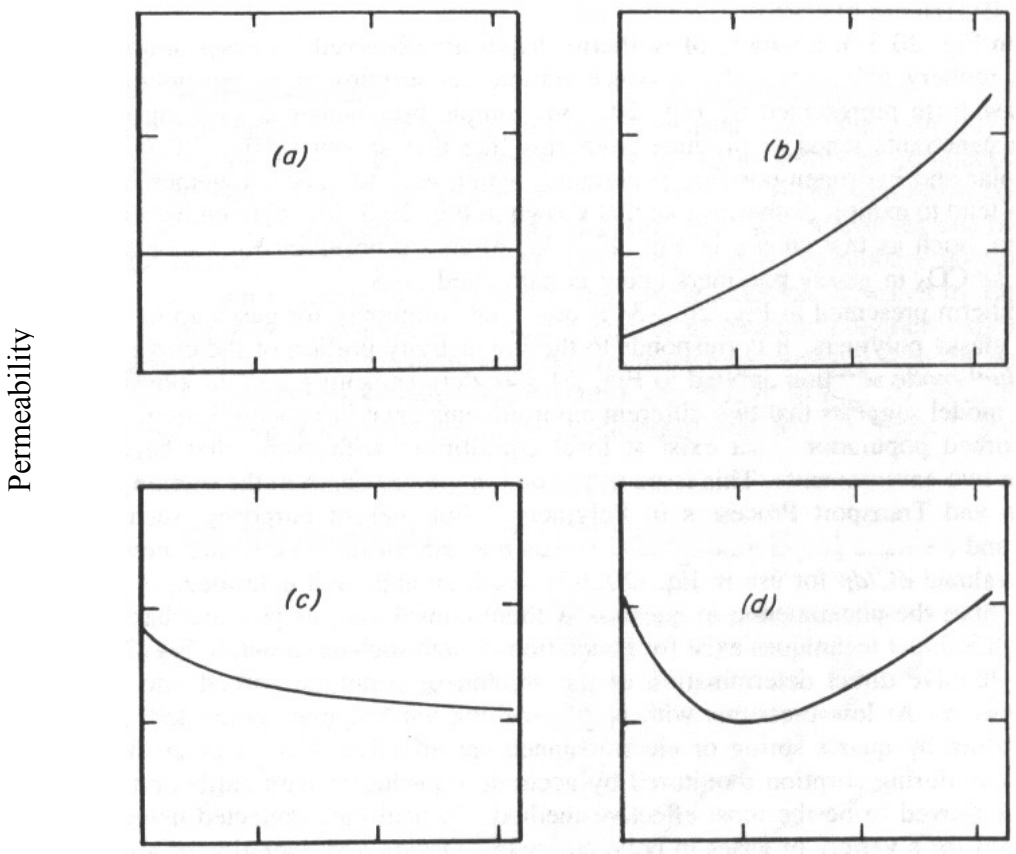

Figure 4. Forms of sorption isotherms observed during gas sorption in polymer membranes *(42)*.

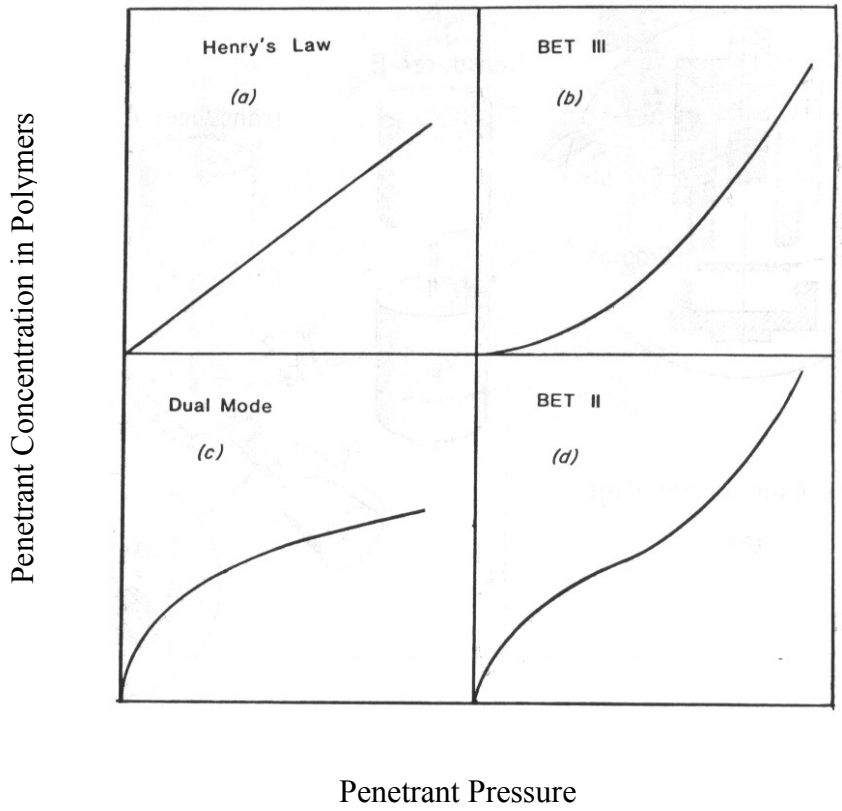

Figure 5. Forms of concentration dependent diffusion coefficients in gas transport through polymer membranes *(42)*.

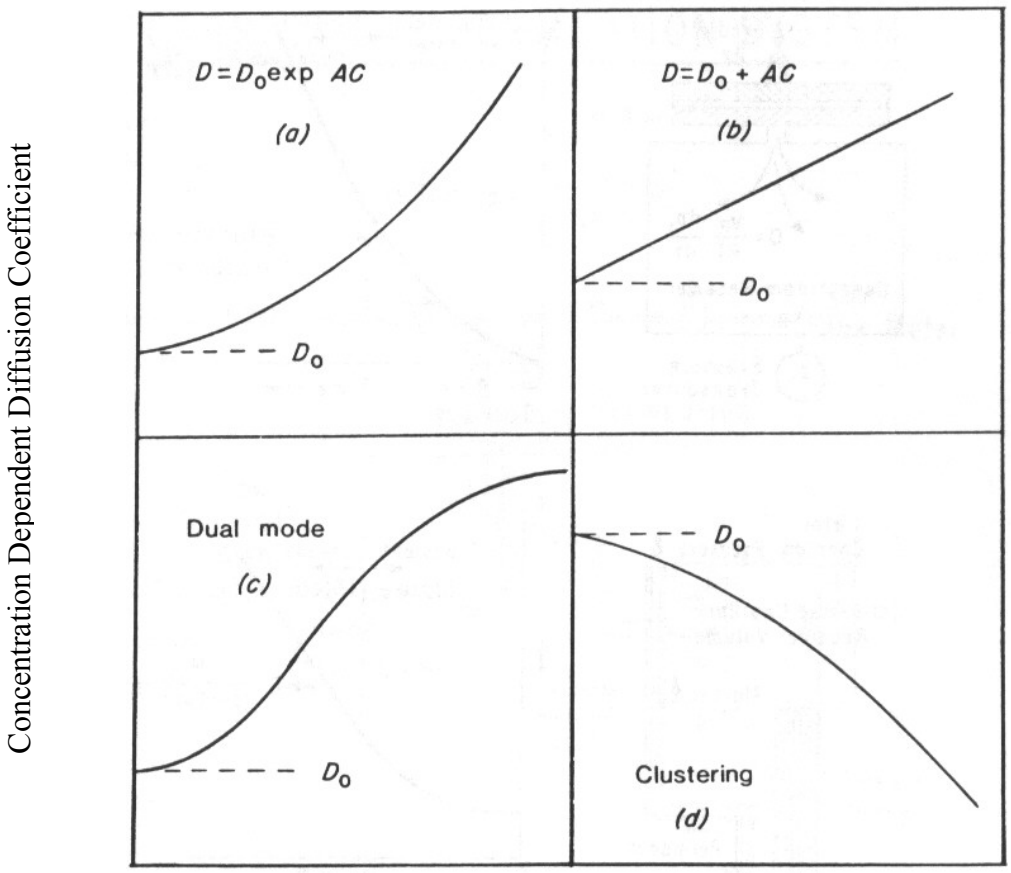

Figure 6. Dow manometric permeability cell. (A) Upper plate; (B) lower plate; (C) rubber gasket; (D) porous filter paper supporting sample film; (E) swivel bolts; (F) mercury storage reservoir; (G) calibrated portion of instrument; (H) Kovar seals; (I) Demi-G valve; (J) gas supply tube; (K) to vacuum; (L) wires to recorder; (M) glass supporting clip *(63)*.

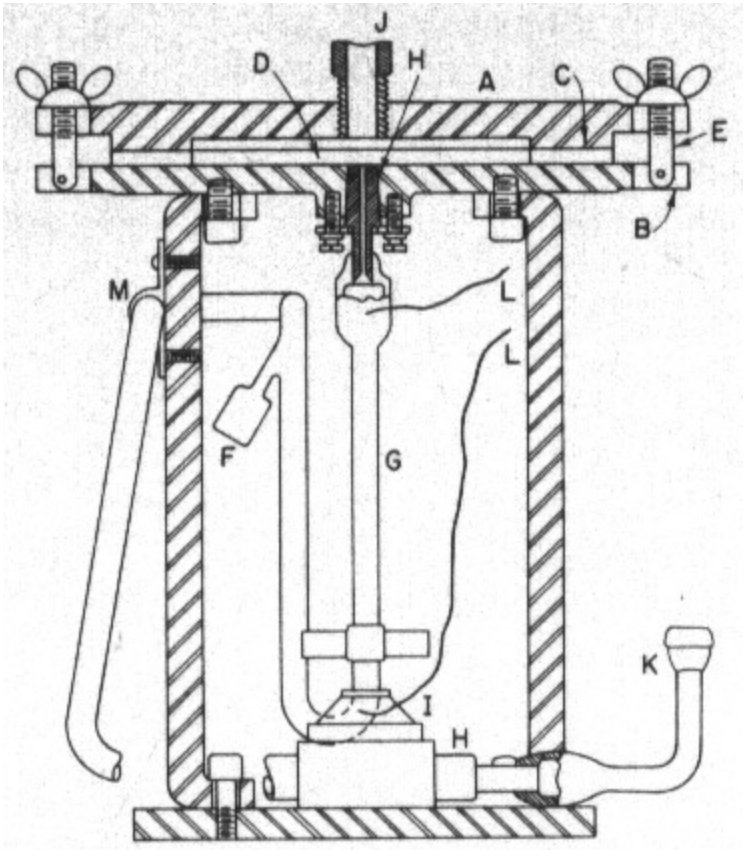

Figure 7. Linde permeation cell *(11)*.

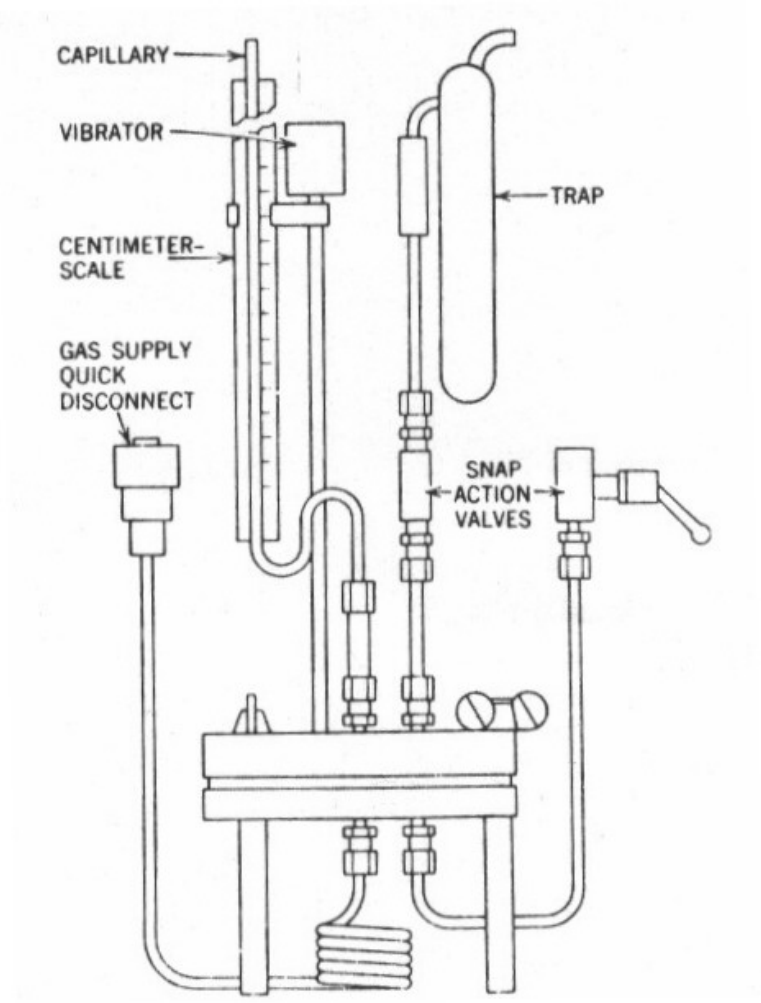

Figure 8. Continuous-flow permeation apparatus *(11)*.

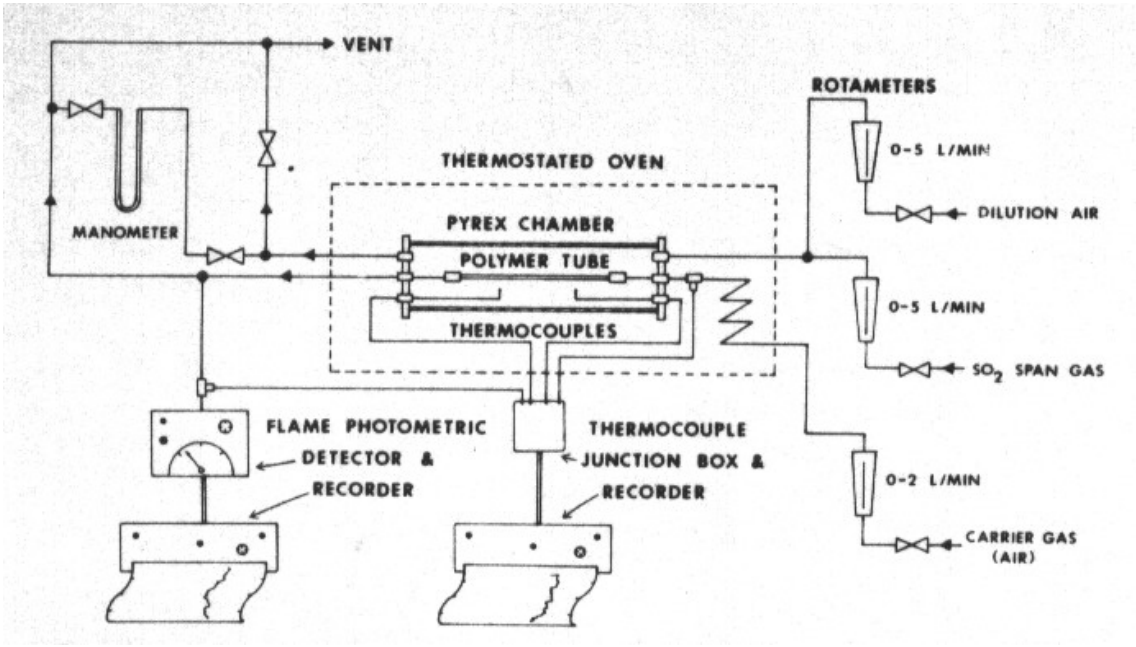

Figure 9. McBain spring balance apparatus *(11)*.

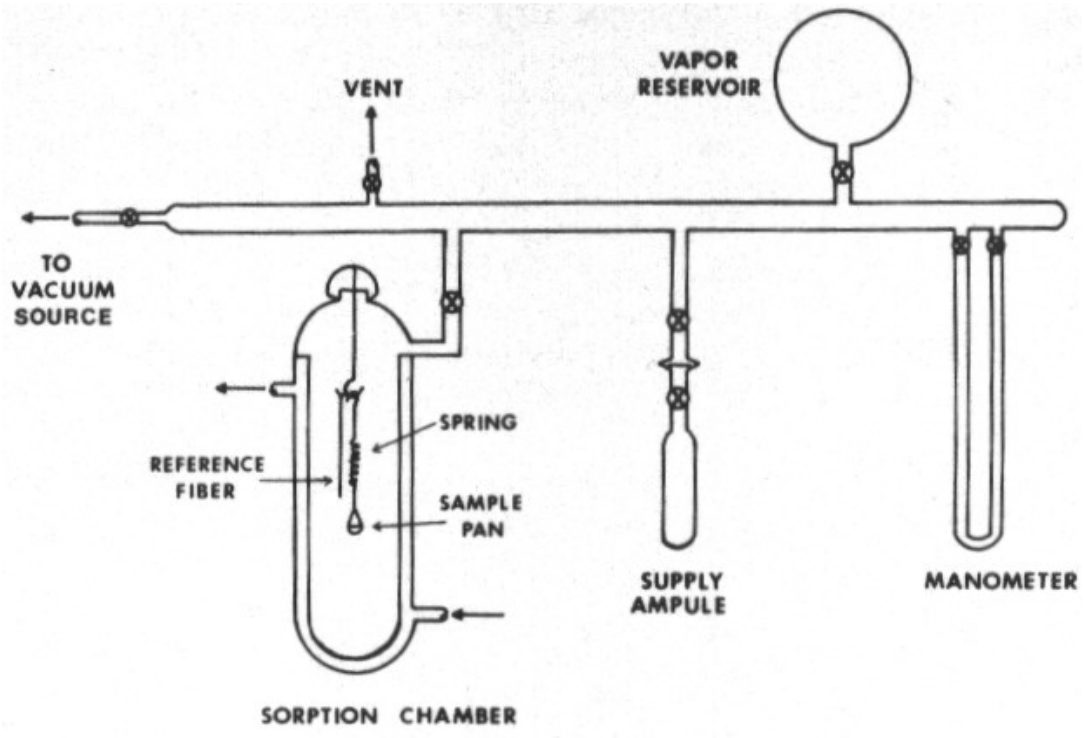

Figure 10. Barometric sorption apparatus *(11)*.

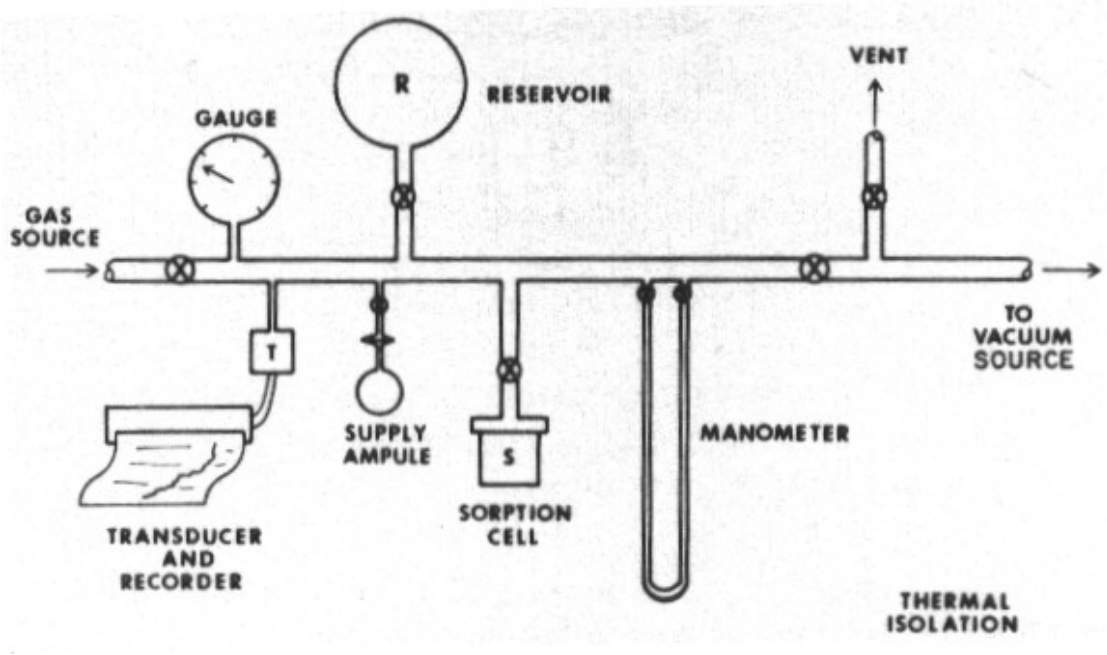

Figure 11. Volumetric sorption apparatus *(11)*.

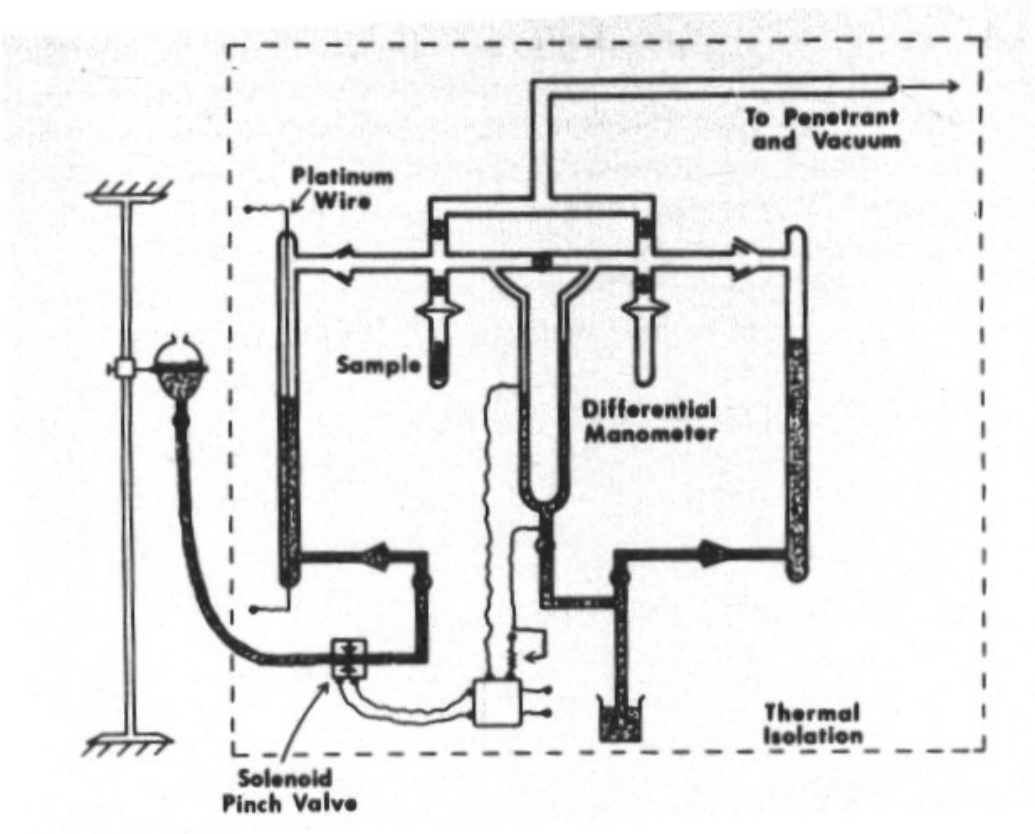

Figure 12. Scheme of a chromatogram peak and its analysis by IGC (*74*).

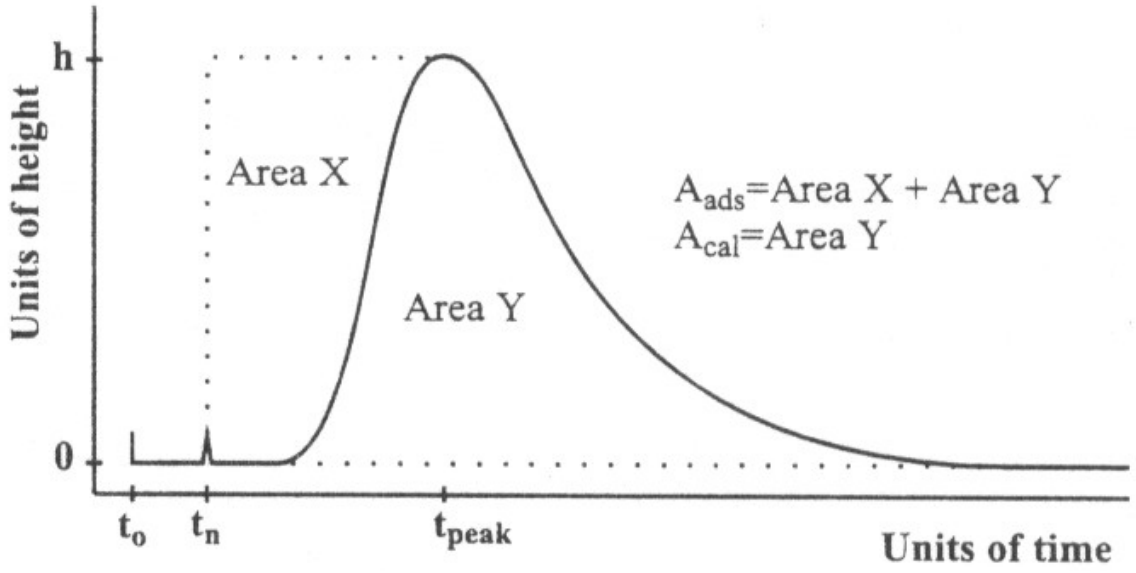

Figure 13. Standard adsorption isotherm for an organic vapor in a food-grade polymer *(92)*.

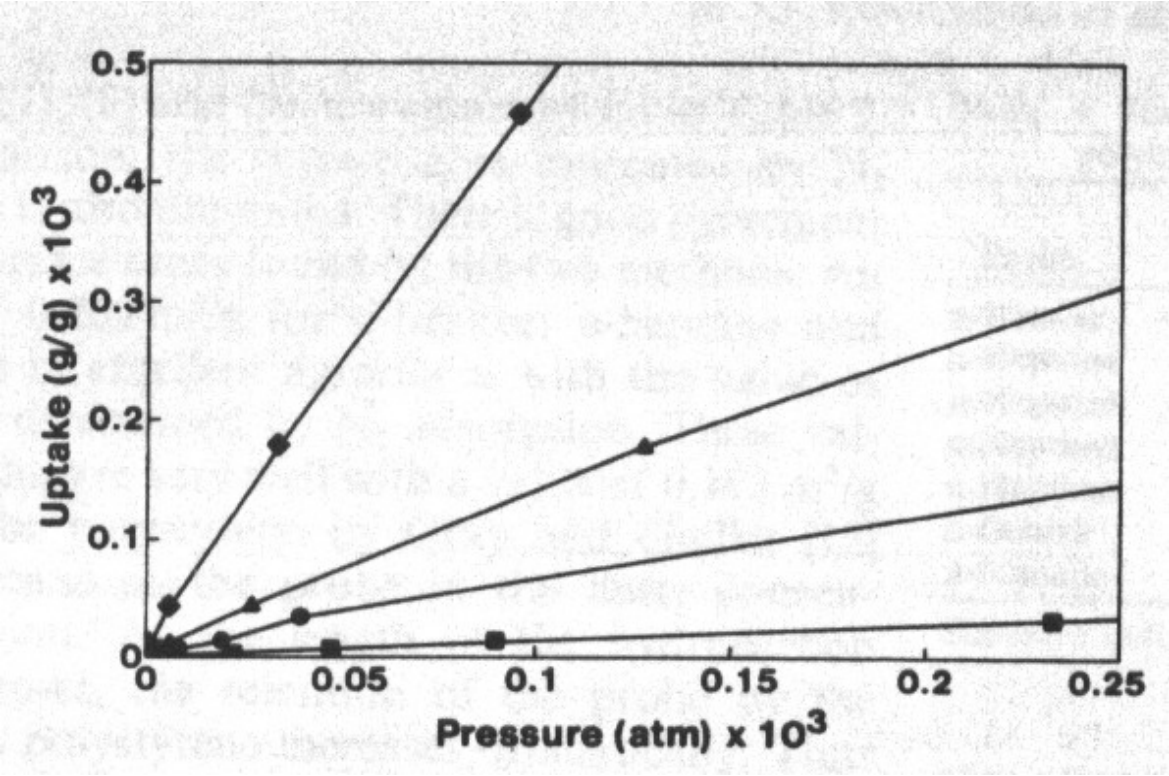

Figure 14. Standard sorption isotherm for an organic vapor in a food-grade polymer *(74)*.